

Bridge Condition Assessment Using Dynamic Response Collected
Through Wireless Sensor Networks

by

Hiwa Fakhraddin Hamid

Submitted in Partial Fulfillment of the Requirements

for the Degree of

Master of Science in Engineering

in the

Civil and Environmental Engineering

Program

YOUNGSTOWN STATE UNIVERSITY

December, 2013

Bridge Condition Assessment using Dynamic Response collected through Wireless
Sensor Networks

Hiwa Fakhraddin Hamid

I hereby release this thesis to the public. I understand that this thesis will be made available from the OhioLINK ETD Center and the Maag Library Circulation Desk for public access. I also authorize the University or other individuals to make copies of this thesis as needed for scholarly research.

Signature:

Hiwa Fakhraddin Hamid, Student

Date

Approvals:

Dr. AKM Anwarul Islam, P.E.
Thesis Advisor

Date

Dr. Javed Alam, Committee Member

Date

Dr. Frank Li, Committee Member

Date

Dr. Sal Sanders
Associate Dean, School of Graduate Studies and Research

Date

ABSTRACT

With a large inventory of deficient and aging bridges in the United States, this research focused on developing dynamic response based health monitoring system of prestressed box beam (PSBB) bridges that will provide more realistic and cost-efficient results. The hypothesis is based on the assumption that the dynamic response is a sensitive and important indicator of the physical integrity and condition of a structure. Two wireless sensor networks (WSNs) were deployed for the collection of real-time acceleration response of a 25-year old PSBB bridge under trucks with variable loads and speeds. The acceleration response of the bridge at its newest condition was collected from the dynamic simulations of its full-scale finite element (FE) models mimicking field conditions. The FE model was validated using experimental and theoretical methods. The acceleration data in time domain were transformed into frequency domain using Fast Fourier Transform to determine peak amplitudes and their corresponding fundamental frequencies for the newest and the current condition of the bridge. The analyses and comparisons of the bridge dynamic response between the newest and the current bridge interestingly indicate a 37% reduction in its fundamental frequency over its 25 years of service life. This reduction has been correlated to the current condition rating of the bridge to develop application software for quick and efficient condition assessment of a PSBB bridge. The application software can instantly estimate overall bridge condition rating when used with the WSN deployed on a PSBB bridge under vehicular loads. The research outcome and the software is expected to provide a cost-effective solution for assessing the overall condition of a PSBB bridge, which helps to reduce maintenance costs and provide technologically improved bridge maintenance service.

Keywords: Prestressed box beam bridge, bridge condition assessment software, health monitoring of bridges, wireless sensor network, bridge maintenance.

ACKNOWLEDGEMENTS

I would like to express my deepest gratitude to my YSU thesis supervisor, Dr. AKM Anwarul Islam, P.E., for his generous support, excellent guidance, valuable remarks and engagement through the learning process of writing this thesis. I would like to thank him for allowing me the opportunity to work with him in this ODOT funded research. This thesis would not have been possible without his continuous encouragement and support.

I would like to extend special thanks to Drs. Javed Alam and Frank Li for serving on my thesis committee and giving me their valuable suggestions over the course of this research. I would also like to express my deepest appreciation to Drs. Scott C. Martin and Daniel H. Suchora for their continuous help and encouragement.

I would like to thank the ODOT, Ohio Highway Patrol and the Mahoning, Ashtabula and Trumbull County personnel for providing materials, drawings, testing tools and equipment, measurements and other important information related to this research. I would like to express my sincere gratitude to Mr. John P. Picuri, P.E., Project Manager, ODOT District 4 Planning and Engineering, for his help with the field tests and valuable suggestions over the duration of this research.

I am grateful to the Higher Committee for Education Development in Iraq for its on-going generosity and support through its scholarship program for my graduate education at YSU.

Finally, I would like to thank my parents, extended family, friends, classmates and the instructors of English Language Institute at YSU for their support and encouragement on my journey through the Civil Engineering graduate program.

TABLE OF CONTENTS

ABSTRACT.....	iii
ACKNOWLEDGEMENTS.....	v
TABLE OF CONTENTS.....	vi
LIST OF FIGURES	ix
LIST OF TABLES.....	xi
Introduction and Literature Reviews	1
1.1 Introduction.....	1
1.2 Problem Statement.....	3
1.3 Literature Reviews.....	5
1.4 Wireless Sensor Technology	7
1.5 Modal Assurance Criterion.....	9
1.6 Research Goals and Objectives	10
1.7 Condition Assessment Procedure	12
Field Data Collection	13
2.1 Bridge Selection	13
2.2 Bridge Descriptions	13
2.3 Types of Truck.....	15
2.4 Wireless Sensor Network	16
2.5 Data Collection.....	20
Finite Element Modeling and Simulation.....	24
3.1 Finite Element Analysis.....	24

3.2	Bridge Modeling and Simulation	25
3.3	Model Assembly.....	29
3.4	Interaction Constraints.....	29
3.5	Moving Load Generation.....	30
3.6	Type of Analysis.....	31
3.7	Job Analysis and Visualization Module	33
	Bridge Condition Assessment.....	35
4.1	Modal Analysis.....	35
4.2	Dynamic Analysis of Beam Systems.....	37
4.3	Fast Fourier Transform.....	39
4.4	Peak-Picking Method	41
4.5	MAC Analysis of Field and Model Data.....	44
4.6	Results	45
4.7	Application Software Algorithms.....	48
4.8	FE Model Validation	56
4.8.1	Experimental Validation	56
4.8.2	Theoretical Validation.....	57
4.9	Application Software and Verification.....	59
4.10	Discussions	63
	Conclusions and Recommendations	65
5.1	Conclusions	65
5.2	Recommendations	67
	References.....	69

APPENDICES	73
APPENDIX A.....	73
APPENDIX B.....	80
APPENDIX C.....	81

LIST OF FIGURES

Figure 2.1: Mahoning Bridge: (a) side view, (b) top view (Google Map).....	14
Figure 2.2: Ashtabula Bridge: (a) side view, (b) top view (Bing Map).....	15
Figure 2.3: Standard dump truck used in this study.....	16
Figure 2.4: SunSPOT hardware kit.....	17
Figure 2.5: Typical configuration of two sets of WSN.....	19
Figure 2.6: Sensor locations on Ashtabula Bridge.....	20
Figure 2.7: Graphical representation of truck path and sensor locations.....	21
Figure 2.8: A test truck approaching to Ashtabula Bridge.	22
Figure 2.9: Acceleration vs. time graphs for sensors in the field.	23
Figure 3.1: Box beams layout plan of Ashtabula Bridge.....	25
Figure 3.2: Typical transverse section of Ashtabula Bridge.....	26
Figure 3.3: Box beam B42-48 cross-section.....	26
Figure 3.4: Meshing and sensor locations on Ashtabula Bridge model.	28
Figure 3.5: (a) Parts and instances and (b) Assembled Ashtabula Bridge model.....	29
Figure 3.6: Ashtabula Bridge model after application of prestress (Exaggerated).....	32
Figure 3.7: Track of a truck load using VDLOAD subroutine.....	32
Figure 3.8: Acceleration vs. time graph for sensors from FE models.	33
Figure 3.9: Natural frequencies and mode shapes of Ashtabula Bridge.....	34
Figure 4.1: Idealization of Ashtabula Bridge.....	37
Figure 4.2: Time Domains and Frequency Domains of some sensors-Field.....	40
Figure 4.3: Time Domains and Frequency Domains of some sensors-FEA.....	40

Figure 4.4: Peak amplitude and its corresponding fundamental frequency-Field.	41
Figure 4.5: Peak amplitude and its corresponding fundamental frequency-FEA.	42
Figure 4.6: Bridge condition assessment input page.	52
Figure 4.7: Bridge condition assessment flow chart.	53
Figure 4.8: Bridge condition assessment flow chart (continued).	54
Figure 4.9: PSBB bridge geometric property.	55
Figure 4.10: Fundamental frequency of Ashtabula Bridge at current condition.	57
Figure 4.11: FE model validation: a) pressure, b) deflected shape (exaggerated).....	58
Figure 4.12: Input Parameters tab of ODOTApp with loaded dynamic response data.	59
Figure 4.13: Bridge Assessment tab of ODOTApp after analysis.....	60
Figure 4.14: Input Parameters tab of ODOTApp with Trumbull Bridge response.	62
Figure 4.15: Output tab of ODOTApp with Trumbull Bridge response.....	62

LIST OF TABLES

Table 1.1: Condition of highway bridges in the U.S.	4
Table 3.1: Properties of box beams and asphalt concrete.....	27
Table 3.2: Properties of reinforcement and prestressing strands	28
Table 4.1: Fundamental frequency and mode shape for beams.....	38
Table 4.2: Bridge peak amplitude-Field	42
Table 4.3: Bridge peak amplitude-FEA	43
Table 4.4: Bridge fundamental frequency-Field.....	43
Table 4.5: Bridge fundamental frequency-FEA.....	44
Table 4.6: Sensors with corresponding MAC values.....	45
Table 4.7: National Bridge Inventory General Condition Rating Guidance	47
Table 4.8: Comparison of results from FEA and approximate calculations.....	58

Chapter 1

Introduction and Literature Reviews

1.1 Introduction

The number of bridges in the United States has been increasing; and bridges have become the lifeline of the nation's transportation infrastructure and commerce. As a bridge ages, it goes through some types of natural deterioration, such as cracking, corrosion, fatigue and other damages that can affect its health and load bearing capacity. The majority of bridges in the United States were built to last around 50 years, and their average age is 42 according to the American Society of Civil Engineers (ASCE) Report Card for America's Infrastructure 2013 (ASCE, 2013). A bridge inspection or condition assessment should be carried out periodically on every bridge to ensure its capacity and safety against current traffic; otherwise, posting, widening, maintenance, rehabilitation, or replacement might be needed.

The health monitoring of bridges includes identifying deficiencies in or current condition of a bridge based on its vibration signatures under vehicular loads. The characteristics of the dynamic response data are very complex to analyze and very challenging to relate to structural health diagnostics, which sometimes require researchers to take different approaches and use diverse methods. The choice of a method over others depends on various factors of a structure, such as age, degree of importance, accessibility, volume of traffic, time, cost, environment, etc.

The current bridge condition assessment consists of visual inspections of bridge components to evaluate their performance and structural integrity. The visual inspection is the primary and the most common method of bridge condition assessment that has been used for decades. The basics of this method depend on noticeable signs of damage and/or distress, such as cracking, spalling, loose connections, deflections, etc. that the structure has experienced over its service life. An inspected bridge is rated from “zero” (failed) to “nine” (excellent) depending on the present physical conditions of its components. However, visual inspection alone, which depends on an inspector’s engineering judgment and visible signs of distress, may not reveal the actual structural condition and deficiencies that are not visible, and/or internal damage the bridge might have undergone over the years. Therefore, the reliability of this method is not well-assured. Moreover, condition assessment based on visual inspection method contains levels of subjectivity and, in some cases, lacks accessibility to critical components of a bridge.

On the other hand, drilling and coring are among the advanced destructive techniques for bridge inspection, which are mostly performed by extracting material samples from bridge elements. These samples are tested in a lab to reveal defects or deteriorations and to determine their properties. These techniques usually cause damages to a structure, and they require repair. Moreover, based on the complexity of a structure, a large number of samples might be needed to assess the health condition of a structure, which in this case is costly and time-consuming.

Non-destructive evaluation techniques including ultrasonic acoustic inspection are local approaches to structural inspection that can be labor-intensive, time-consuming and quite expensive (Lynch, 2005). Moreover, traditional wired sensor networks for health

monitoring of large civil structures require large amounts of coaxial cables that are expensive to install and maintain.

As the volume of traffic and use of bridges in transportation networks have been increasing, a comprehensive health monitoring system is necessary to ensure adequate public safety. The wireless sensor network (WSN) technology may provide such public safety by detecting damage and assessing health condition of structures at earlier stages. This method has attracted researchers in developing new tools for assessing condition of bridges using advanced communication technology. The primary goal of this research is to develop a tool that will help ODOT and other state Departments of Transportation (DOTs) save time and money in assessing the health of bridges.

1.2 Problem Statement

According to the U.S. Department of Transportation (USDOT), out of around 607,380 bridges across the country, 66,749 (11%) were categorized as structurally deficient, and 84,748 (13.9%) were categorized as functionally obsolete, and our infrastructure received a grade of ‘D⁺’ with bridges having a grade of ‘C⁺’ (ASCE, 2013). A structurally deficient bridge may be closed or restricted to traffic in accordance with weight limits because of limited structural capacity. In order to ascertain public safety, limits for speed and weight on these bridges must be posted. According to the National Bridge Inventory Standards (NBIS), bridges are considered structurally deficient if general condition rating of a bridge component is 4 or less according to the Federal Highway Administration (FHWA, 2004). Functionally obsolete bridges may have design features and geometrics that do not meet current bridge standards. Bridges with narrow

lanes and shoulders, and inadequate vertical clearance are some examples of functionally obsolete bridges. These bridges are not unsafe, but they cannot accommodate current traffic volumes, vehicle sizes, and weights. In order to keep these bridges open to traffic, they need to be brought up to the current standards.

From 2004–2009, the number of deficient bridges in rural areas declined by 12,763. However, in urban areas during the same time frame, there was an increase of 4,098 in the number of deficient bridges (USDOT, 2010). In 2009, 23% of rural bridges were deficient, while in urban areas the number was 30%. The statistics of deficient bridges in the rural and urban areas from 2004 to 2009 are shown in Table 1.1 (USDOT, 2010).

Table 1.1: Condition of highway bridges in the U.S.

	2004	2005	2006	2007	2008	2009
No. of bridges, Total	593,813	595,363	597,340	599,766	601,396	603,259
Urban	137,598	142,408	146,041	151,171	153,407	156,305
Rural	456,215	452,955	451,299	448,595	447,989	446,954
Structurally deficient bridges, Total	77,752	75,923	73,784	72,520	71,461	71,177
Urban	12,175	12,600	12,585	12,951	12,896	12,828
Rural	65,577	63,323	61,199	59,569	58,565	58,349
Functionally obsolete bridges, Total	80,567	80,412	80,317	79,804	79,933	78,477
Urban	30,298	31,391	32,292	33,139	33,691	33,743
Rural	50,269	49,021	48,025	46,665	46,242	44,734

The American Association of State Highway and Transportation Officials (AASHTO) estimated in 2008 that roughly \$140 billion is needed to repair every deficient bridge in this country – about \$48 billion to repair structurally deficient bridges and \$92 billion to improve functionally obsolete bridges (AASHTO, 2008). The cost of eliminating all existing bridge deficiencies as they arise over the next 50 years is estimated to be \$850 billion dollars in 2006, equating to an average annual investment of \$17 billion (NSTP, 2007). Through the Federal-Aid Highway Act of 1968 and its subsequent revisions, the FHWA requires all publicly owned highway bridges longer than 20 ft located on public roads to be inspected and evaluated following NBIS recommended procedures (FHWA, 2004).

In Table 1.1, it is shown that a large amount of nation's bridges is structurally deficient or functionally obsolete, and deterioration of bridges is a continuous process. Therefore, the development of modern tools and methods for bridge condition assessment is vital to bridge maintenance. Response-based condition assessment of bridges may provide more realistic results compared to current methods. In this research, the overall structural condition of a prestressed box beam (PSBB) bridge under moving loads has been assessed based on its real-time dynamic response collected through WSN.

1.3 Literature Reviews

Bridges are very critical parts of a transportation network, and therefore, the structural health monitoring (SHM) of bridges is vital for maintaining such networks of roads and highways. The main objective of SHM herein is to estimate the loss of structural integrity due to aging, environment and increase in traffics, which can

adversely affect the performance of a structure. Consequently, these causes reduce the load bearing capacity of bridges. Concrete degradation, steel corrosion, change in boundary conditions, and weakening of connections in structures over time are major concerns in bridge structures. If bridge damage remains unattended, its structural integrity and service capability worsen over time. Therefore, frequent condition assessment of bridges is vital in maintaining a healthy transportation network. The condition assessment of a bridge based on its dynamic response can be effective in early detection of damage in a bridge. Lynch, *et al.* (2006) monitored the performance of Guemdang Bridge, South Korea, using a dense network of 14 high-resolution wireless sensors. Also installed in parallel was a commercial tethered monitoring system. They collected acceleration response of the bridge under forced vibrations induced by a calibrated 40-ton truck at 40, 60 and 80 kmph speed by using both tethered and WSNs. They used MAC for statistical analyses and compared the results from both systems. The performance of the less expensive wireless monitoring system was shown to be comparable to that of the tethered counterpart. Samali, *et al.* (2003) described field-testing of more than 20 timber bridges across New South Wales, Australia. The bridge assessment procedure involved the attachment of accelerometers underneath bridge girders. The vibration response and natural frequency of the bridge superstructure was measured when a “calibrated sledgehammer” was used to hit the unloaded deck, and then again with a relatively small mass applied at mid-span. The difference in dynamic response allowed them to calculate the in-service flexural stiffness of each bridge. Some of the work that has been cited by FHWA is mentioned herein.

Cawley and Adams (1979) related changes of successive mode frequencies to the existence and location of structural deterioration in beams. Salawu and Williams (1995a) reported a study of the forced vibrations of a bridge before and after repair. The test results demonstrated the changes in natural frequency induced by the repair. Mazurek and DeWolf (1990) showed in laboratory tests that changes in support condition and crack development affect natural frequencies and modal amplitudes (FHWA, 2005).

The literature reviews show the use and importance of dynamic response in damage detection and bridge condition assessment. Therefore, it can be concluded that further study is needed to relate the dynamic response of a bridge to its amount of deterioration and the current condition. The dynamic loading, WSN, and acceleration data collected on bridges have been used in these past studies in damage detection and health monitoring, and were helpful for the scope of this research. The goal of this study is to develop a tool for condition assessment of a PSBB bridge by analyzing its dynamic response, such as acceleration, collected through WSN under moving loads.

1.4 Wireless Sensor Technology

With the advancement in wireless communication technology and its capability of health monitoring of structures, the use of wireless sensors in SHM has become an effective choice to reduce maintenance cost, and to increase public convenience and safety. The wireless sensor technology allows the use of networks of sensors over a structure to collect its dynamic response. The sensors can be installed at locations that are difficult to access during other methods of health assessment. In this method, the installation and labor costs of wireless sensors are minimal while an efficient and

accurate condition assessment is achieved in a short period of time. The wireless sensor communication technology for health monitoring of structures was proposed by Straser and Kiremidjian (Straser, *et al.*, 1998). Even though it is challenging to measure the true behavior of a structure using this approach (Doebbling, *et al.*, 1996), Kim, *et al.* (2007) deployed a 64-node WSN, distributed over the 4,200 ft long main span of the Golden Gate Bridge in San Francisco, with the goal of identifying initial issues with WSN in monitoring structural health and ambient vibrations. Gangone, *et al.* (2008) deployed a 20-node WSN in Potsdam, New York, which also supported strain gages apart from accelerometers. Both efforts were able to capture important modes of dynamic bridge behavior that agrees with theoretical results.

The bridge condition assessment can be performed using various methods. The time, cost, and reliability of each method are different from others. The major concern or challenge for researchers is to find a method that is time- and cost-efficient, and reasonably accurate in detecting deficiencies in bridges. The WSN technology may provide such opportunities in overcoming these challenges. The use of WSN technology was simple and fast, and yet efficient in collecting real-time dynamic response of bridges in this research. The sensors were placed at various critical locations on the bridge to capture the response of the whole bridge under variable moving loads at various speeds. The traffic was only closed for a short period of time. No damage was caused to the bridge, and no maintenance was required after performing the test using this method. Therefore, it appears that SHM using WSN may become a cost-effective and efficient method for the condition assessment of bridges to their owners.

1.5 Modal Assurance Criterion

The modal assurance criterion (MAC) analysis is a modal analysis technique that estimates the degree of correlation between two mode shape vectors. Most often, it is used to check the correlation between the mode shapes obtained from experiments and analytical models. It was proposed by Allemang and Brown (Allemang and Brown, 1982) with MAC values ranging from 0 to 1. A MAC value close to 1 indicates well-correlated modes, whereas a value close to zero shows little or no correlation between two modes.

The MAC can be mathematically summarized by the following Eq. 1.1 (Allemang and Brown, 1982):

$$MAC(\{\phi_A\}_m, \{\phi_B\}_n) = \frac{|\{\phi_A\}_m^T \{\phi_B\}_n|^2}{(\{\phi_A\}_m^T \{\phi_A\}_m \{\phi_B\}_n^T \{\phi_B\}_n)} \quad (1.1)$$

Where, $\{\phi_A\}_m$ = mode shape of model A, $\{\phi_A\}_m^T$ = transpose of mode shape of model A, $\{\phi_B\}_n$ = mode shape of model B, $\{\phi_B\}_n^T$ = transpose of mode shape of model B.

The MAC analysis has been widely used in research as an efficient tool. Allemang (2002) reviewed the use of MAC over a period of 20 years. Some of the works that have been cited are mentioned herein. Yuan, *et al.* (2009a) used MAC to optimally place sensors on a cable-stayed bridge, whereas Caponero, *et al.* (2002) used an interferometer and MAC for identification of component modes. Desforges, *et al.* (1996) used MAC for tracking modes during flutter testing, while Heylen and Janter (1989) applied MAC for dynamic model updating (Marwala, 2010).

The development of MAC over the last several decades has led researchers to use a number of similar assurance criteria for determining the degree of correlation between experimental and analytical modes of a structure. The application of MAC principle can

be extended in several ways. Some of other extensions and similar assurance criteria of MAC are: Weighted Modal Analysis Criterion (WMAC), Partial Modal Analysis Criterion (PMAC), Modal Analysis Criterion Square Root (MACSR), Scaled Modal Analysis Criterion (SMAC), Coordinate Modal Assurance Criterion (COMAC), Modal Assurance Criterion with Frequency Scales (FMAC), Modal Assurance Criterion Using Reciprocal Vectors (MACRV), Enhanced Coordinate Modal Assurance Criterion (ECOMAC), Frequency Domain Assurance Criterion (FDAC), Frequency Response Assurance Criterion (FRAC), Complex Correlation Coefficient (CCF), Modal Correlation Coefficient (MCC), Coordinate Orthogonality Check (CORTHOG) (Allemang, 2002).

The use of the modal assurance criterion, and the development and use of a significant number of related criteria, has been remarkable and is most likely due to the overall simplicity of the concept (Allemang, 2002). Some of the typical uses of MAC analysis are correlation with analytical modal models (mode pairing), structural fault/damage detection, quality control evaluations, and optimal sensor placement. Due to its importance in modal correlation and damage detection, MAC analysis was used in this research to find the degree of correlation between the dynamic response of a real bridge and its finite element (FE) bridge models.

1.6 Research Goals and Objectives

PSBB bridges have been used since the middle of the last century (around 1950) in the United States (NCHRP, 2009). These bridges constitute about 26 percent of bridges in the State of Ohio according to NBI data (FHWA, 2012). The span limit for PSBB bridges usually ranges from 15 to 100 ft, although span lengths up to 120 ft have been

designed and constructed. This type of bridge is not normally used for four-lane divided highways or where the one way design average daily truck traffic (ADTT) exceeds 2,500 (ODOT, 2011). The objective of this research is to develop a tool for the overall condition assessment of a PSBB bridge using the WSN technology. To achieve the stated objective, each of the two single-span PSBB bridges in Ohio were equipped with two sets of WSN for collecting real-time acceleration data under trucks at various speeds and weights. The hypothesis is based on the assumption that the dynamic response is a sensitive and important indicator of the physical integrity and condition of a structure. The perception of the researchers includes that the global response of a bridge to vehicular loads is directly related to its overall structural health. Therefore, the present health condition of a bridge can be assessed from the analysis of its dynamic response under moving loads.

The application software for the condition assessment of PSBB bridges is developed under this research. This tool can be quickly deployed in the field to instantly estimate overall condition rating of a PSBB bridge by collecting real-time dynamic response and by customizing necessary parameters of the bridge. This novel approach of assessing global bridge condition may fundamentally change the current approach of bridge condition assessment, which depends on external inspection of bridge components. The current method does not reveal hidden structural damages and/or deterioration of bridge components due to vehicular and environmental distress over its lifespan. The research outcome and the application software can be very useful, time- and cost-efficient, and will increase public convenience and safety.

1.7 Condition Assessment Procedure

The following steps were followed to accomplish this response-based condition assessment:

- Develop wireless sensor networks to collect the real-time acceleration response of the bridge under moving trucks in the field.
- Perform Fast Fourier Transform (FFT) on the acceleration data in time domain, and determine peak amplitudes and their corresponding fundamental frequencies of the current bridge.
- Build full-scale finite element 3D models of the bridge from its original construction drawings, which represents the bridge at its newest condition (right after construction).
- Run simulations of the bridge models under the same loads mimicking the field conditions in order to determine the peak amplitudes and corresponding fundamental frequencies of the model bridge.
- Establish a relationship between the dynamic response of the bridge at its newest and current conditions, and correlate it to the standard general condition ratings (GCR) of bridges established by National Bridge Inventory (NBI) to assess the structural condition of a bridge.

Chapter 2

Field Data Collection

2.1 Bridge Selection

Adjacent prestressed box beam bridges are widely used in new bridge construction and have many advantages over other bridge types due to speed and ease of construction, aesthetics, span to depth ratio and cost. Although early construction practices may have led to serviceability issues, improved practices have made the box girder bridge a viable, cost-effective structural system (Prestressed Concrete Institute, 2009). In this study, three PSBB bridges were selected from a list of available PSBB bridges in ODOT District 4. Priority was given to bridges with more years in service, longer spans, lower traffic, and closer to the YSU campus. Two of the bridges were used for data collection and modeling, while the third one was used for validation of the application software developed using the dynamic response from the first two bridges.

2.2 Bridge Descriptions

The first selected PSBB bridge, as shown in Fig. 2.1, was constructed in July 1993 in the Mahoning County, Ohio. It is a simply supported single span composite PSBB bridge with average daily traffic of 5,400. The bridge structural reference number is MAH-45-0579, and it crosses over the West Branch of the Meander Creek on the S. Salem-Warren/ Route 45 with a 30° skew in the horizontal alignment. The length of the

bridge is 84.5 ft, and the width is 44 ft. It consists of 11 adjacent 48 in. wide and 42 in deep PSBBs. A concrete deck of 5.5 in. is laid on the top of the box beams. The beams are transversely connected through 18 in. thick equally spaced concrete diaphragms and staggered tie rods. The bridge has two 12 ft wide traffic lanes with 10 ft wide shoulders on both sides. Steel railings are attached on the exterior edges of the bridge.



Figure 2.1: Mahoning Bridge: (a) side view, (b) top view (Google Map).

The second bridge, built in July 1988, is a fixed-supported single span PSBB bridge with structural reference number ATB-322-1916, which crosses over the Pymatuning Creek on Highway 322 in Ashtabula County, Ohio. The bridge, as shown in Fig. 2.2, is 85 ft long and 36 ft wide. It consists of nine adjacent PSBBs supported on concrete abutments at both ends. The box beams are 48 in. wide and 42 in. deep with a 2.5 in. thick layer of asphalt concrete on top. Three equally spaced 18 in. thick concrete diaphragms and staggered tie rods transversely connected the box beams together. The horizontal alignment of the bridge is straight with no skew. The bridge has two 12 ft wide

traffic lanes, and two 6 ft wide shoulders. Steel railings are attached on both exterior edges of the bridge.



Figure 2.2: Ashtabula Bridge: (a) side view, (b) top view (Bing Map).

2.3 Types of Truck

Three standard dump trucks provided by the Mahoning and Ashtabula County Engineers Offices were used to produce vibrations on both bridges. A standard dump truck used in this study is shown in Fig. 2.3. The truck axle loads and dimensions were measured by the Ohio State Highway Patrol. The axle dimensions of the three trucks were the same; however, their weights were different. The trucks had an axle distance of 14.9 ft between the front and rear axles, and 6 ft track width. Three different truck weights were used in this study, which were Empty Truck, Half-loaded Truck, and Fully-loaded Truck. The axle loads and dimensions data sheet of each truck is attached in Appendix A.



Figure 2.3: Standard dump truck used in this study.

2.4 Wireless Sensor Network

The structural condition of each bridge is estimated herein from the vibration signatures of the selected bridges under vehicular loads. The algorithms for condition assessment were developed from the real-time acceleration response of the bridge under moving trucks collected through WSN. The sensor set-up and data collection procedures for both bridges were similar. However, in the Mahoning Bridge, the glue used to attach the sensors on the bridge deck did not cure enough to make the sensors integral with the bridge due to the near-freezing temperature during data collection. It was suspected that the uncured glue might have absorbed part of the bridge vibrations leading the vibration data unacceptable for further consideration. Therefore, vibration data collected on Ashtabula Bridge were only considered for analysis and modeling.

The acceleration response of Ashtabula Bridge was recorded using two sets of WSN deployed simultaneously on the bridge under trucks with various weights and speeds. Each set of WSN included four wireless accelerometer sensors and one base station connected via a Universal Serial Bus (USB) cable to a laptop. The Sun Small Programmable Object Technology (SunSPOT) sensors were used in this research and a typical package is shown in Fig. 2.4.



Figure 2.4: SunSPOT hardware kit.

Each SunSPOT sensor has a unique 16-digit media access control address and can capture vibration data in all three different axes simultaneously, although acceleration in Z-axis (vertical direction) only was collected for this research. Collected time-stamped data for each sensor can be easily separated for further analysis. Even though the sensors

are equipped with built-in rechargeable batteries, yet they were charged with external power supplies throughout the entire test using USB cables. The accuracy of the sensor data was very important; therefore, the accelerometers were calibrated and customized in a lab environment before deploying them on the field.

The wireless sensors and base stations have generic Java embedded development platforms. Programs were written by using Java Integrated Development Environment to customize them for deploying in the field for data collection. In this research, eight sensors with two base stations were used to build two WSNs. The base station in WSN 1 collected data only from sensors 1 to 4 while the base station in WSN 2 collected data from sensors 5 to 8 only. These sensors were customized in such a way that they transmitted data only to the assigned base station. The laptop connected to the base station collected and recorded vibration data for further processing. A typical configuration of two sets of WSN is shown in Fig. 2.5. Both WSNs were set to collect data at a sampling rate of 100 Hz at 2g scale.

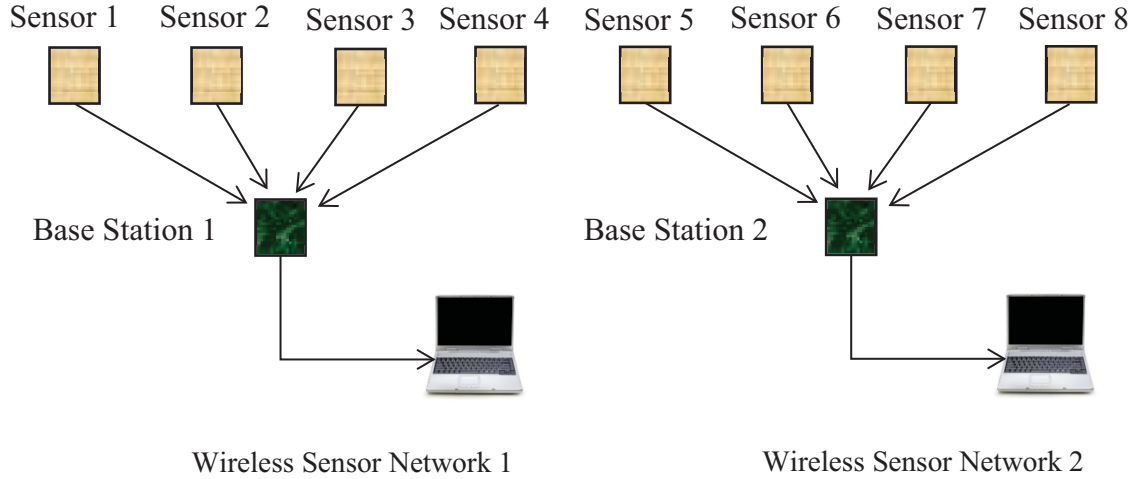


Figure 2.5: Typical configuration of two sets of WSN.

All eight sensors were placed in the left traffic lane at 8 ft from the longitudinal centerline, and symmetrically about the transverse centerline of the bridge at 5 ft spacing between adjacent sensors. Installation of the sensors and their locations on the bridge are shown in Fig. 2.6. The sensors were marked from 1 to 8 in the direction of the moving truck. Sensor locations were marked and cleaned before attaching sensors on the bridge deck using quick-setting glue to prevent loss of bridge vibration. Glued interfaces between sensors and bridge deck were checked before data collection and found stiff enough not to absorb bridge vibration.



Figure 2.6: Sensor locations on Ashtabula Bridge.

2.5 Data Collection

The accelerometer sensor captures analog acceleration signals due to forced vibrations of the bridge from vehicular movement, converts them to digital format with an analog-to-digital converter (ADC), and transmits the digital data directly to the base station. As stated earlier, three different truck weights, namely Empty Truck (E), Half-loaded Truck (H), and Fully-loaded Truck (F), were used to produce bridge vibrations. Each truck was run at 10, 15, 20, and 25 mph. The truck runs were named as E10, E15, E20, E25, H10, H15, ..., F10, F15, and so on. The bridge was closed to traffic during data collection to ensure data integrity and safety to researchers.

To evenly distribute the effect of the truck load across the bridge width, each truck was driven on the centerline of the bridge. The collection time for all sensors was set to 10 seconds based on the bridge length and truck speed. This time consisted of the time the truck needed to pass over the bridge plus extra time accounted for the effects of the truck approaching and exiting the bridge. The graphical representation of the truck path and sensor locations is shown in Fig. 2.7.

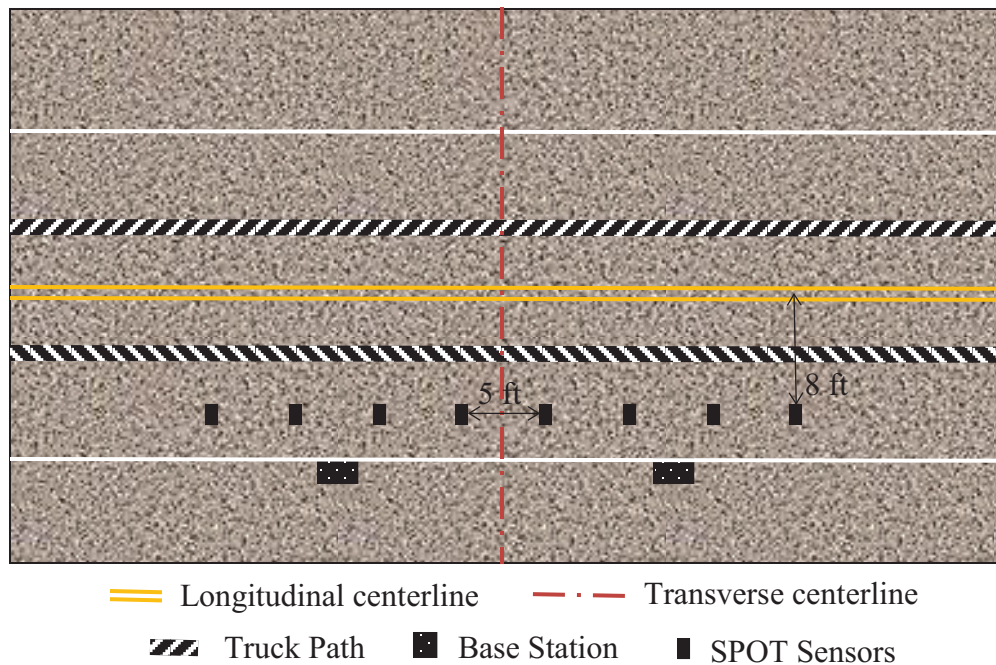


Figure 2.7: Graphical representation of truck path and sensor locations.

During each truck run at a specific speed, the first base station received collected acceleration data from Sensors 1 to 4 and transmitted to the first laptop, while the second base station received collected acceleration data from Sensors 5 to 8 and transmitted to the second laptop.

The data collection started with the Empty Truck at 10 mph and acceleration data were collected simultaneously by both WSNs. The trucks maintained their assigned

constant speed during the entire 10-second duration for all runs. After a successful completion of the first run, the second, third, and fourth runs were performed with the same truck at 15, 20, and 25 mph, respectively. The same procedures were followed for the next eight runs with the Half-loaded and Fully-loaded Trucks. Figure 2.8 shows one of the trucks approaching the bridge, and driving over the bridge centerline.



Figure 2.8: A test truck approaching to Ashtabula Bridge.

Every single run produced 8 subsets of sensor data. For 12 runs with 3 weights and 4 speeds, a total of 96 subsets of acceleration data were collected from the Ashtabula Bridge. A part of acceleration data captured from the bridge under the Half-loaded Truck at 25 mph is shown in Appendix B.

Both laptops saved all acceleration data received from the base stations using Microsoft Excel comma separated value (CSV) format. Sample real-time acceleration vs. time graphs for some sensors are shown in Fig. 2.9.

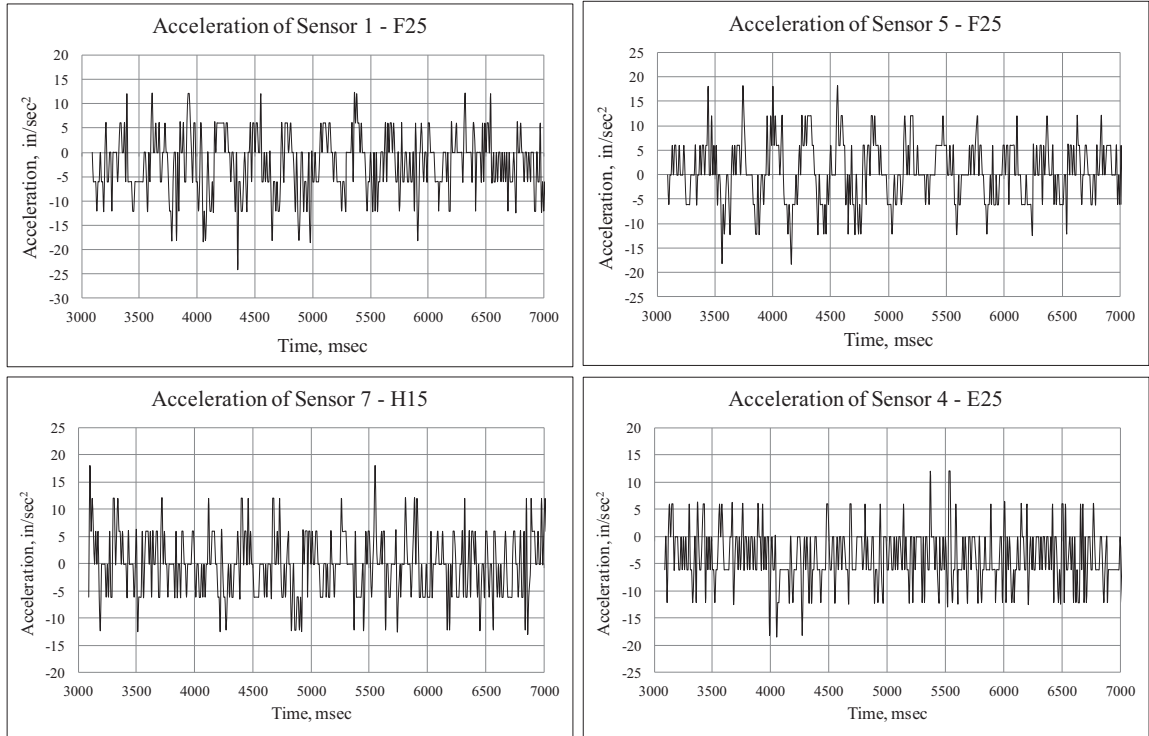


Figure 2.9: Acceleration vs. time graphs for sensors in the field.

Chapter 3

Finite Element Modeling and Simulation

3.1 Finite Element Analysis

The finite element analysis (FEA) is a numerical technique, which is used to model and solve complex engineering problems in a virtual environment. With the advancement in technology and dramatic increase in computer processing capacity, FEA has become a dominant and reliable method for solving a variety of problems numerically that would otherwise require expensive experimental testing.

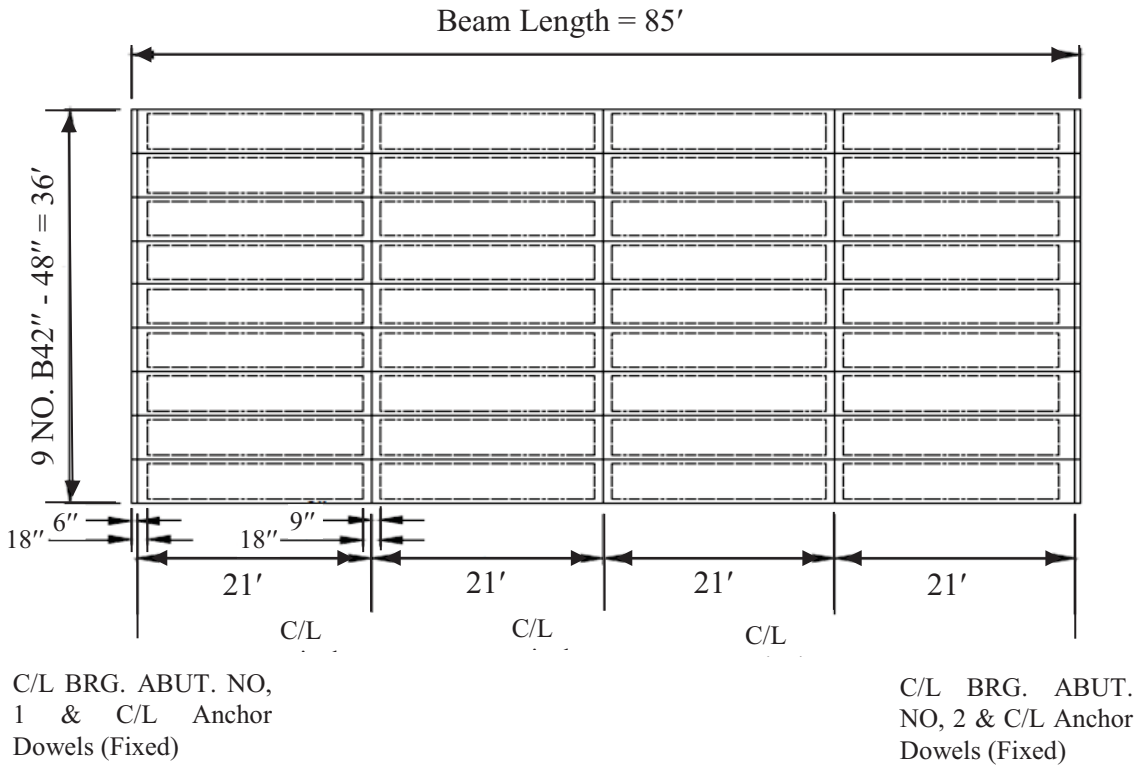
In this study, the FEA software ABAQUS 6.12 (SIMULIA, 2013) was used to build a full-scale 3D finite element model of Ashtabula Bridge. The model represents the bridge at its newest condition right after it was opened to traffic.

ABAQUS includes three main parts for analysis and simulation, which are ABAQUS CAE, ABAQUS/Standard, and ABAQUS/Explicit. ABAQUS CAE provides a simple interface for creating a wide range of shapes and structures, submitting and monitoring jobs, and evaluating the results from ABAQUS/Standard and ABAQUS/Explicit simulations. The modeling consistency in ABAQUS CAE makes it an easy-to-use and yet highly productive and attractive tool for FEA users. Some of the common modules in ABAQUS CAE are: Part, Material, Section, Assembly, Steps, Field Output Requests, Interactions and Constraints, Loads, BCs, Mesh, Job Analysis, and Post-Processing. Both ABAQUS/Standard and ABAQUS/Explicit are supported within

the ABAQUS CAE modeling environment, and they are designed to provide the user with two complementary mechanisms.

3.2 Bridge Modeling and Simulation

The Ashtabula Bridge was modeled based on ODOT drawings shown in Figs. 3.1 to 3.3. The bridge model has four main parts: box beams, wearing surface, steel reinforcement, and prestressing strands. Each of these parts was modeled separately, and they were assembled to build the complete bridge model. Constraints and interactions between the part instances were added as necessary to account for the contact and bond



properties.

Figure 3.1: Box beams layout plan of Ashtabula Bridge.

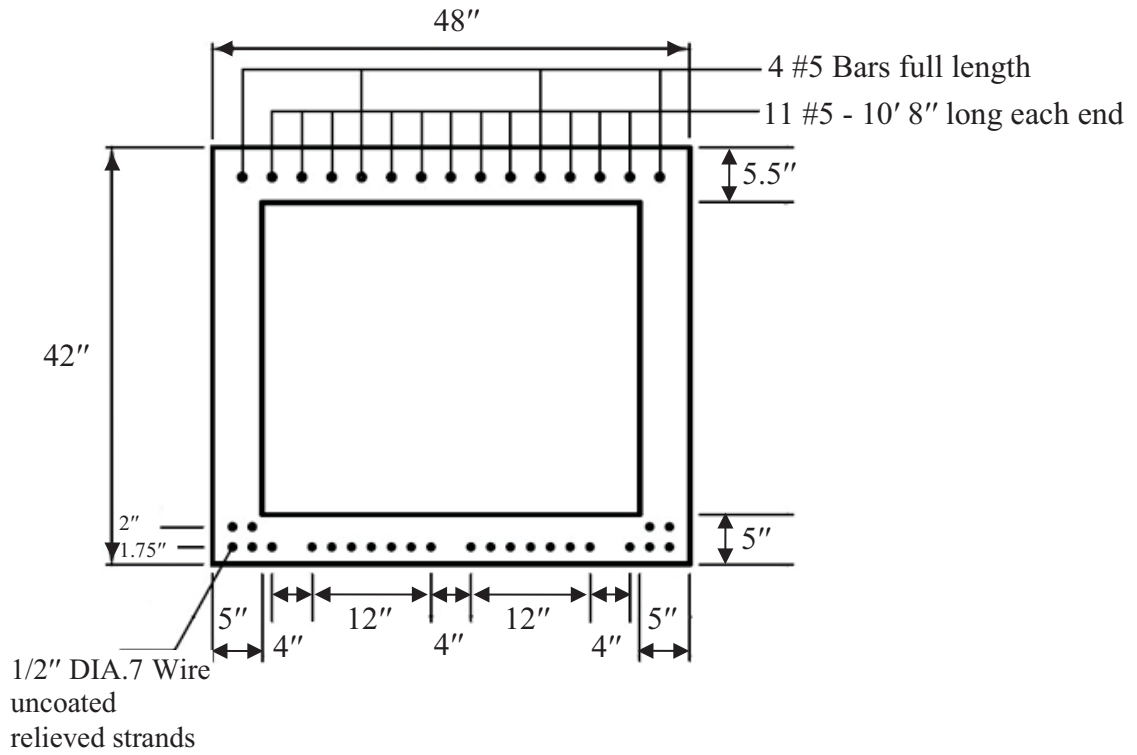


Figure 3.2: Typical transverse section of Ashtabula Bridge.

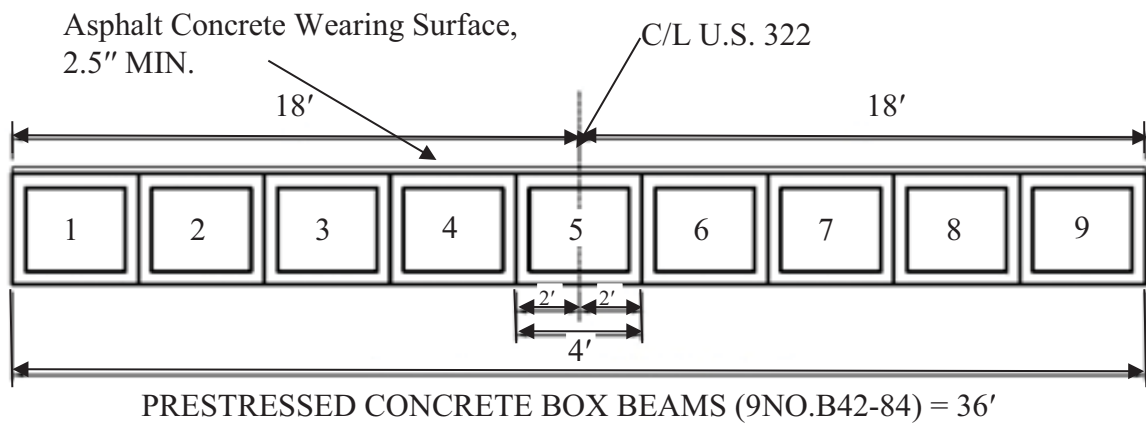


Figure 3.3: Box beam B42-48 cross-section.

The bridge consists of nine adjacent PSBBs with a 2.5 in. thick asphalt concrete wearing surface overlay. The properties of the box beams and the wearing surface are shown in Table 3.1. The box beams and the asphalt concrete wearing surface were modeled as 3D-deformable solid shapes using three-dimensional first-order hexahedral 8-node solid elements.

Table 3.1: Properties of box beams and asphalt concrete

Parts	Unit weight (lb/ft ³)	Modulus of Elasticity (psi)	Poisson's Ratio
Box beams	150	4496060.776	0.15
Asphalt concrete	150	350000	0.35

A reasonable fine mesh of 10 in., as shown in Fig. 3.4, was used for the box beams and the wearing surface. For the purpose of convergence check, another model with 5 in. mesh size was created to ensure the 10 in. mesh size was reasonable.

The exact locations of the eight sensors during the field test were mimicked in the bridge simulation, and are shown in red dots in Fig. 3.4. In the post-processing module after the complete analysis of the bridge, the acceleration data at each sensor point were collected and saved for further analysis.

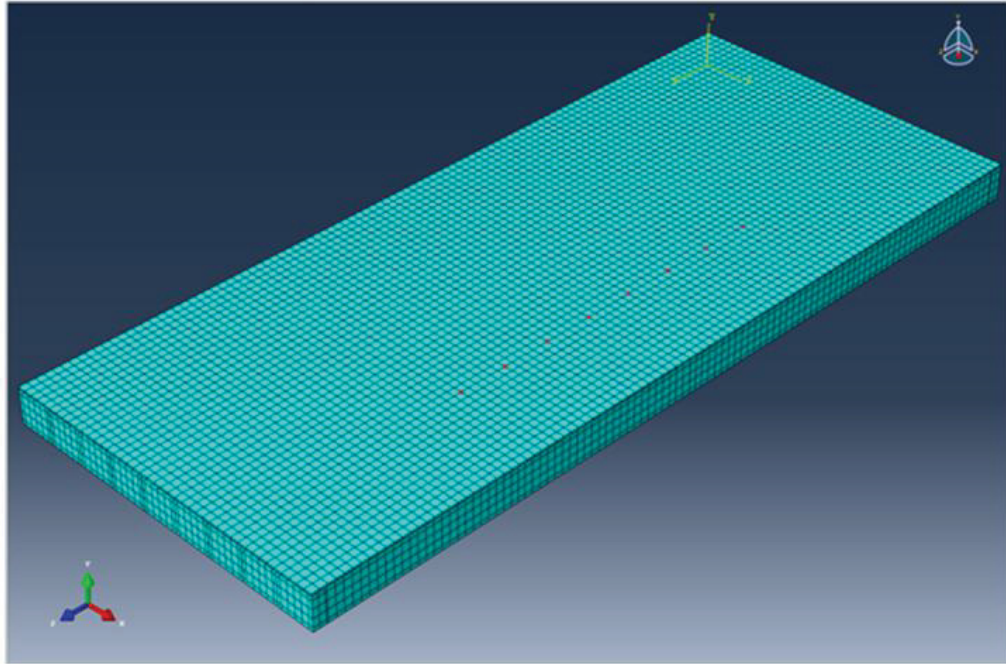


Figure 3.4: Meshing and sensor locations on Ashtabula Bridge model.

Since the contribution of the reinforcement to the overall stiffness of the bridge was very small, truss element was used for the modeling the steel reinforcement and the prestressing strands with 10 in. mesh size. The properties of the reinforcement and prestressing strands are shown in Table 3.2.

Table 3.2: Properties of reinforcement and prestressing strands

Parts	Unit weight (lb/ft ³)	Modulus of Elasticity (psi)	Poisson's Ratio
Reinforcement	490	29000000	0.3
Prestressing strands	490	28500000	0.3

3.3 Model Assembly

Bridge parts were modeled separately as part instances and the bridge model was created by assembling the part instances. The assembly of the bridge parts is shown in Fig. 3.5.

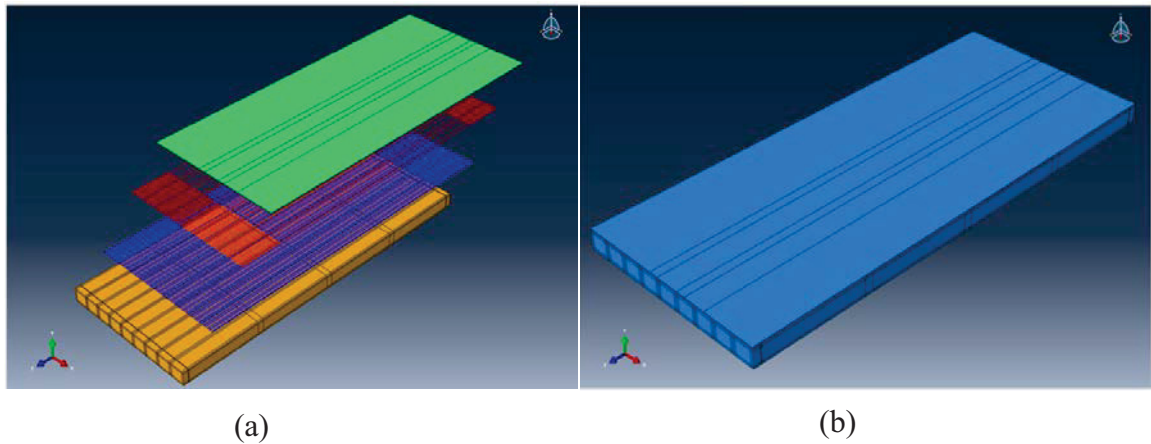


Figure 3.5: (a) Parts and instances and (b) Assembled Ashtabula Bridge model.

3.4 Interaction Constraints

The mechanical contact between part instances or regions of an assembly is not recognized in ABAQUS unless that contact is specified in the Interaction module. Three different kinds of interactions, as explained below, were used in the bridge modeling.

A tie constraint ties two separate surfaces (master and slave) together so that there is no relative motion between them. Due to the gravitational load and the full surface contact, a tie constraint was used between the box beams and the wearing surface. The box beams were defined as the master surfaces while the wearing surface was defined as the slave surface. The slave surface follows the master surface in all directions.

The steel reinforcement and prestressing strands were embedded inside the concrete box beams so that they undergo the same strain or deformation as the surrounding concrete under loads.

The bridge was built with nine PSBBs arranged in a side-by-side pattern and transversely connected together by concrete diaphragms and staggered tie rods. Frictional forces develop between the contact surfaces of the concrete box beams, which resist the relative tangential motion of the beams. According to the American Concrete Institute (ACI) Building Code Section 11.6.4.3 (ACI, 2008), the coefficient of friction was taken as 0.6λ , where $\lambda=1.0$ for normal weight concrete. Since the box beams were made of normal weight concrete, the friction coefficient of 0.6 was used as the interaction friction property between the concrete box beams.

3.5 Moving Load Generation

The VDLOAD user subroutines written in FORTRAN were used to define the moving truck loads as functions of position, time, velocity, etc. A FORTRAN compiler is required to compile and link user subroutines to the ABAQUS bridge models. A total of 12 VDLOAD user subroutines were written for 12 truck runs. Each subroutine was customized for the specific truck weight and speed. According to the American Association of State Highway and Transportation Officials (AASHTO) Bridge Design Specifications Section 3.6.1.2.5, the tire contact area of the truck wheels was assumed as a single rectangle with 20 in. width and 10 in. length (AASHTO, 2007). The front and rear wheel loads of each truck were then applied as uniformly distributed pressure over

the contact area. The truck moving load was applied on the centerline of the bridge mimicking the field runs.

3.6 Type of Analysis

The bridge was analyzed for static and dynamic loads. ABAQUS/Standard was used to analyze the static prestress on the box beams while ABAQUS/Explicit was used to analyze the dynamic truck loads on the bridge.

ABAQUS/Standard is an ideal environment, which is well-suited to simulate static and low-speed dynamic functions when accurate stress solutions are of main interest. On the other hand, ABAQUS/Explicit is an efficient tool that provides accurate solutions for high-speed, transient, highly discontinuous, large, and non-linear dynamics simulations. The results at any point within an ABAQUS/Standard can be used as the starting conditions for continuation in ABAQUS/Explicit. Similarly, an analysis that starts in ABAQUS/Explicit can be continued in ABAQUS/Standard as well. The flexibility provided by this integration allows ABAQUS/Standard to be applied to those portions of the analysis that are well-suited to an implicit solution technique (SIMULIA, 2013).

In this research, both ABAQUS/Standard and ABAQUS/Explicit were used together to analyze the dynamic response of Ashtabula Bridge under the moving trucks. The bridge model was analyzed for static loading with the initial prestress of 27.1 kips per strand calculated from ODOT bridge drawings. Figure 3.6 shows the bridge model under the effect of the prestress.

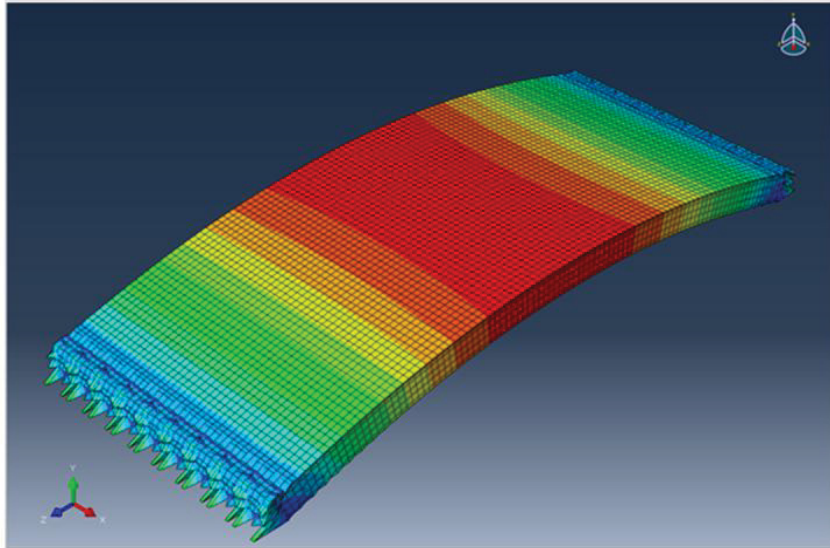


Figure 3.6: Ashtabula Bridge model after application of prestress (Exaggerated).

The results from the prestressed model were used as the starting conditions in ABAQUS/Explicit. The prestressed model was defined as an initial step in the dynamic analysis model, where the truck loads were applied on the bridge. The truck path was defined, and the truck load was applied on the whole path as shown in Fig. 3.7.

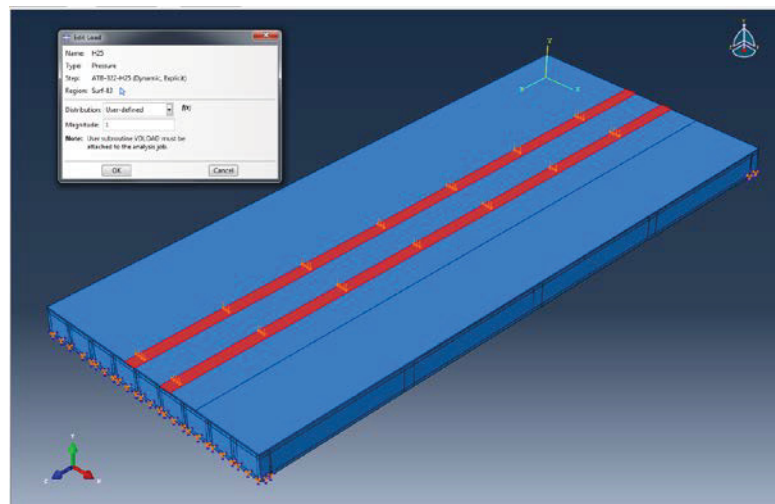


Figure 3.7: Track of a truck load using VDLOAD subroutine.

3.7 Job Analysis and Visualization Module

Dynamic simulations of FEA models are very time-consuming, which result from the size and type of the model, meshing size, analysis type, and the computer capacity. In this study, two very powerful desktop computers were used for analysis and simulation of the bridge models.

The Job module was used to analyze each of the 12 models created in ABAQUS/CAE. The Job module allows creating a job or multiple jobs for a model, submitting it for analysis, and monitoring its process. In this module, each of the user subroutine files, created in FORTRAN for various truck load scenarios, was imported and linked to its corresponding model. Graphs in Fig. 3.8 show the acceleration responses from the finite element models at various sensor locations.

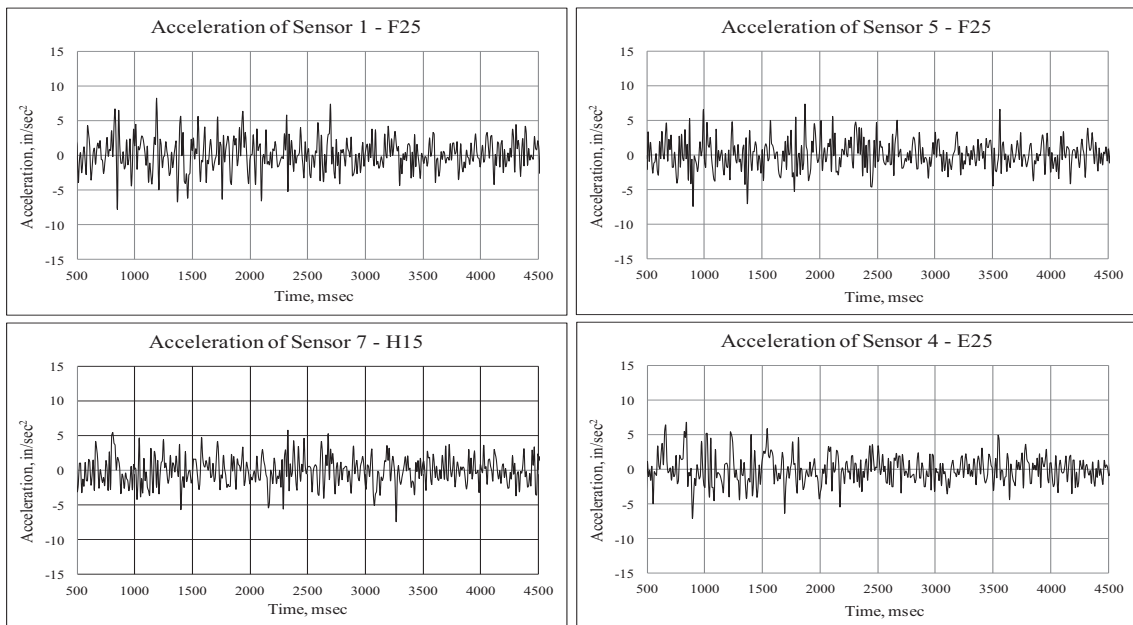


Figure 3.8: Acceleration vs. time graph for sensors from FE models.

The frequency analysis was also performed to extract the natural frequencies and their corresponding mode shapes of the bridge. The frequency analysis was later used in validating the FE model of the bridge. ABAQUS/Standard provides three eigenvalue extraction methods: Lanczos, automatic multi-level sub-structuring (AMS), and subspace iteration. The Lanczos method was used to perform the frequency analysis to find the first four natural frequencies and their corresponding mode shapes, as shown in Fig. 3.9.

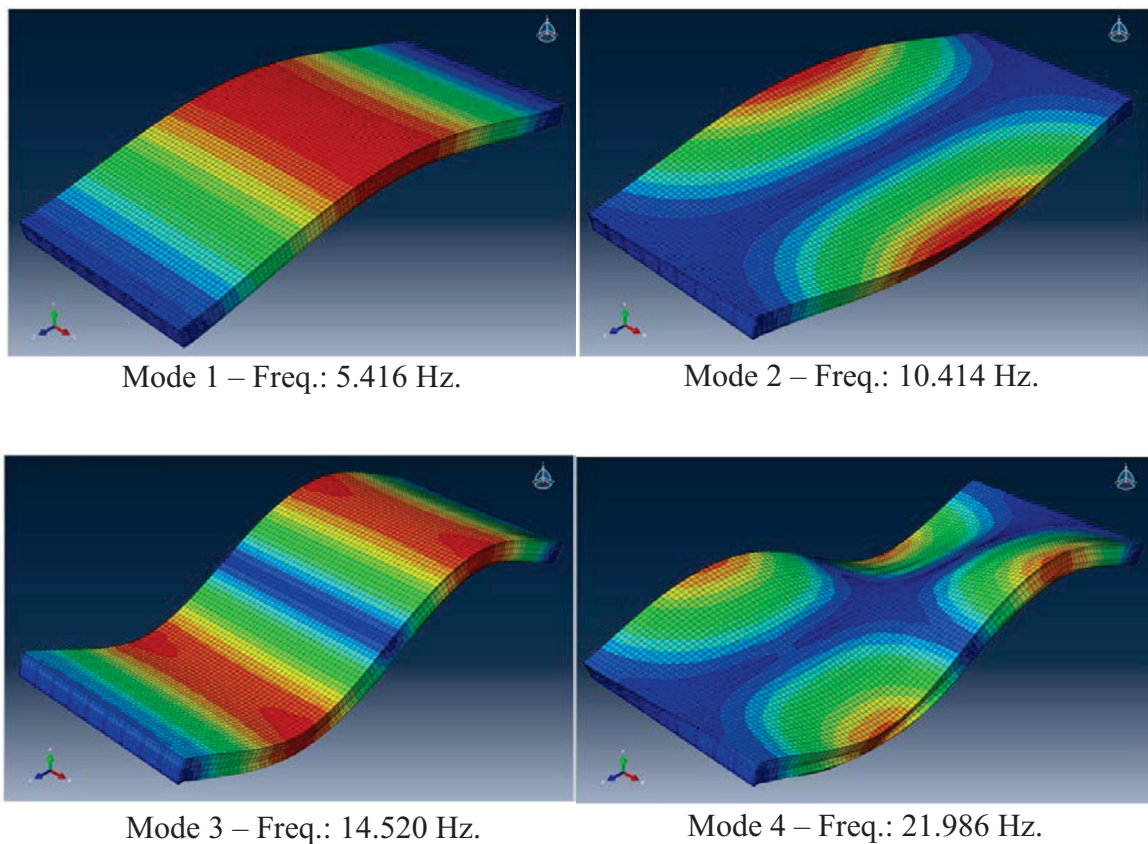


Figure 3.9: Natural frequencies and mode shapes of Ashtabula Bridge.

Chapter 4

Bridge Condition Assessment

4.1 Modal Analysis

The modal analysis is performed on a structure under dynamic conditions in terms of its frequency, damping, and mode shapes. The vibration amplitude in a structure diminishes if the excitation forces are removed. The reduction in vibration amplitude is caused by the damping forces. The simulation of damping mechanism, however, is beyond the scope of this study. On the other hand, the frequencies and mode shapes of a structure are affected by its mass and stiffness. The mass of a structure does not change significantly over time when there is no big loss in the cross-section of the structure. In the Ashtabula Bridge, no significant loss in the cross-section was noticed. Therefore, it was assumed that the mass of the bridge did not change over time. The variable that plays important role in the health of a structure is the stiffness or the flexural rigidity, which can be determined from the geometric and material properties of the structure. The stiffness of a structure decreases over time due to deterioration and cracks, which in turn decrease the capacity of the structure. Moreover, the natural frequency of a structure is directly proportional to the square root of stiffness. Therefore, any change in stiffness causes change in frequency and the capacity or health of the structure. By determining the change in dynamic properties, such as frequency, in a structure between its newest and current conditions, the amount of damage and the health condition of the structure

can be estimated. The dynamic properties of a system under vibration can be determined analytically using modal analysis, as shown in the following discussions.

From the theory of structural dynamics, the equation of motion of any linearly elastic system subjected to external dynamic force can be described by the following equation:

$$[M]\{\ddot{x}\} + [C]\{\dot{x}\} + [K]\{x\} = \{f(t)\} \quad (4.1)$$

Where, $[M]$ = mass matrix, $[C]$ = damping matrix, $[K]$ = stiffness matrix, $\{f(t)\}$ = nodal force vector, $\{x\}$ = nodal displacement vector, $\{\dot{x}\}$ = nodal velocity vector, $\{\ddot{x}\}$ = nodal acceleration vector.

In case of a force-free vibration, $\{f(t)\} = 0$, Eq. 4.1 can be expressed by Eq. 4.2.

$$[M]\{\ddot{x}\} + [C]\{\dot{x}\} + [K]\{x\} = 0 \quad (4.2)$$

After some simple calculations, the natural circular frequency (ω) of the system can be expressed by Eq. 4.3.

$$\omega = \sqrt{\frac{k}{m}} \quad (4.3)$$

The modal frequency, f , of a system is equal to its circular frequency divided by 2π , and is given by Eq. 4.4.

$$f = \frac{1}{2\pi} \sqrt{\frac{k}{m}} \quad (4.4)$$

4.2 Dynamic Analysis of Beam Systems

Idealizing a complex real structure into a simplified system is an essential part in the theory of structural engineering. Continuous systems with distributed mass have an infinite number of degrees of freedom and an infinite variety of deformation patterns. Analyzing a system with such complexities is impractical. In this study, the bridge was idealized as a beam, as shown in Fig. 4.1, with distributed mass and elasticity and fixed-fixed support condition for dynamic analysis.

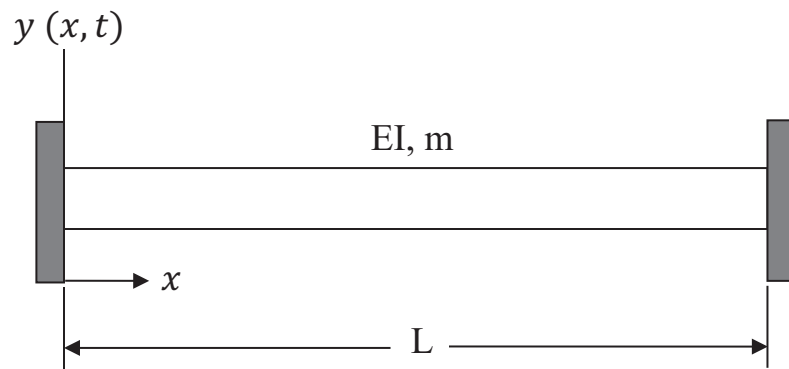


Figure 4.1: Idealization of Ashtabula Bridge.




The vertical deflection of the beam can be defined in term of distance and time by Eq. 4.5.

$$y(x, t) = \phi(x) f(t) \quad (4.5)$$

Here, x = distance along the length of the beam, y = vertical deflection, t = time, $\phi(x)$ = shape function.

By solving Eq. 4.5, the fundamental frequency of the beam can be found. Table 4.1 shows the fundamental frequency and mode shape for beams with different support conditions (Paz, 1985).

Table 4.1: Fundamental frequency and mode shape for beams

Support Condition	Fundamental frequency, Hz	Mode shape
Fixed-Fixed	$f = 3.5608 \sqrt{\frac{EI}{mL^4}}$	
Fixed-Hinged	$f = 2.4529 \sqrt{\frac{EI}{mL^4}}$	
Simply Supported	$f = 1.5708 \sqrt{\frac{EI}{mL^4}}$	

Where, f = fundamental frequency, E = Young's modulus of elasticity, I = moment of inertia, m = mass per unit length of the beam, and L = length of the beam.

The fundamental frequency of the bridge at its current condition can be determined by analyzing the real-time acceleration data collected on the bridge from the field dynamic loading procedure, as shown in Chapter 2. On the other hand, the fundamental frequency of the bridge at its newest condition can be found from the FEA or theoretical analysis shown in Table 4.1. The change in frequency between its newest and current conditions indicates the amount of deterioration of the bridge occurred over its life time. The type and location of damage are beyond the scope of this study; rather the overall change in frequency and amount of deterioration are the main focus. From this change,

the overall structural condition of the bridge is estimated and correlated to the general condition rating of the bridge.

4.3 Fast Fourier Transform

The acceleration data collected at the sensor locations on the bridge are time-dependent. The peak amplitude and its corresponding fundamental frequency, however, were needed to assess the overall structural condition of the bridge. Therefore, the acceleration data in the time domain need to be transformed into the frequency domain to determine the peak amplitudes and their corresponding frequencies. This transformation of the time domain data can be performed by Discrete Fourier Transform using the Fast Fourier Transform (FFT) algorithm developed and proposed by Cooley and Tukey in 1965 (Cooley and Tukey, 1965). The FFT requires the number of data points to be of power of 2, such as 256, 512, or 1024. Figures 4.2 and 4.3 show the time domain and corresponding frequency domain data from the field and the FEA bridge models, respectively.

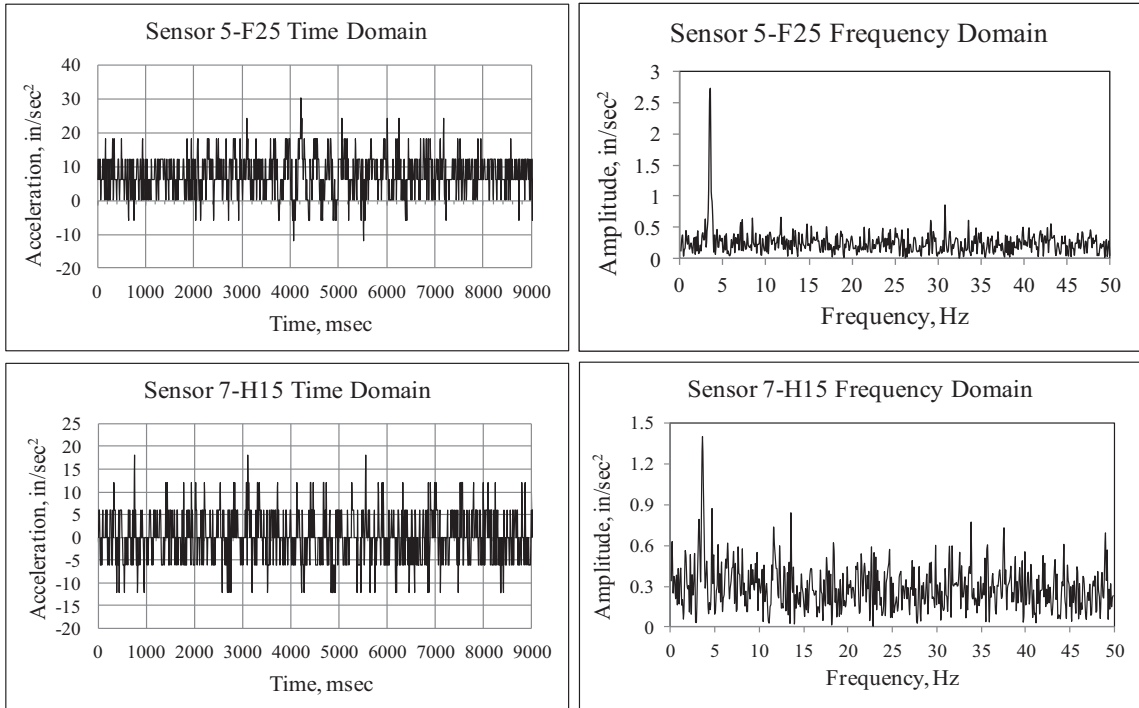


Figure 4.2: Time Domains and Frequency Domains of some sensors-Field.

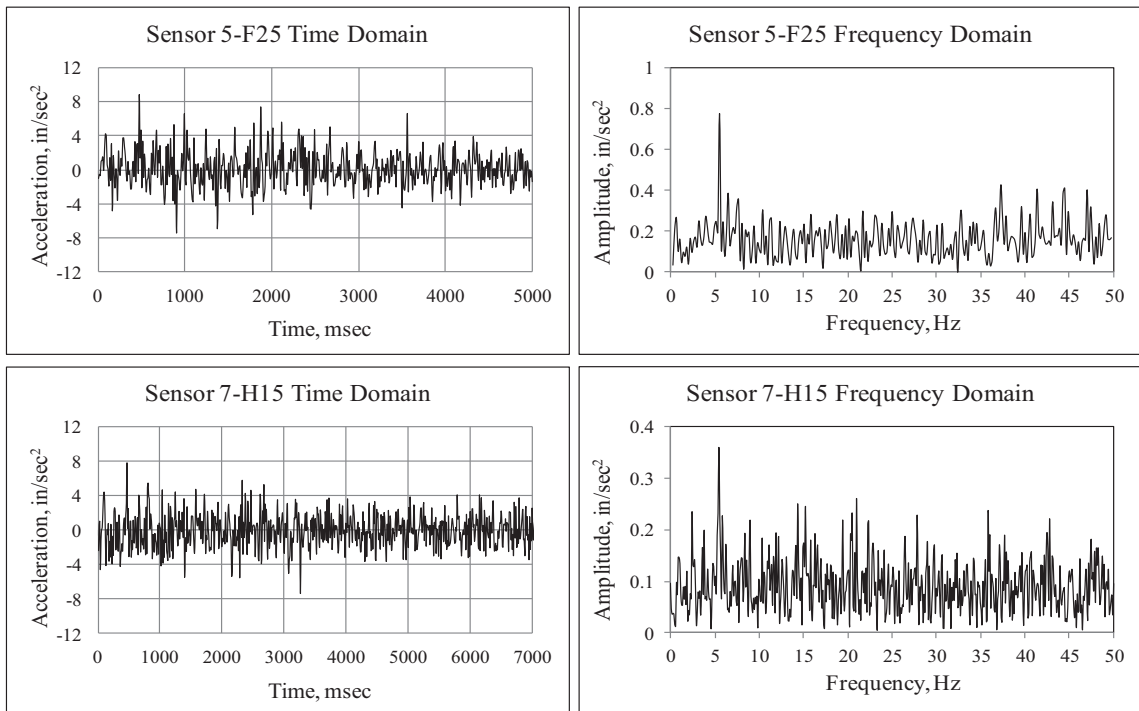


Figure 4.3: Time Domains and Frequency Domains of some sensors-FEA.

4.4 Peak-Picking Method

In the frequency domain, the peak-picking method was used to select the peak amplitudes and their corresponding fundamental frequencies. The peak-picking is a fast method for the identification of the modal characteristics of a bridge. It is a nonparametric method, which is mostly used in the frequency domain. The concept of this method is based on the fact that the frequency response of a structure goes through peak values around the natural frequencies (Ren, *et al.*, 2003). The frequencies at these peak values are a good estimate for fundamental frequencies of the system. The fundamental frequency of the bridge was determined as the frequency corresponding to the first dominant peak amplitude. Figures 4.4 and 4.5 show the peak-picking method in selecting the peak amplitudes and their corresponding fundamental frequencies at various sensor locations from the field and the FEA bridge models, respectively.

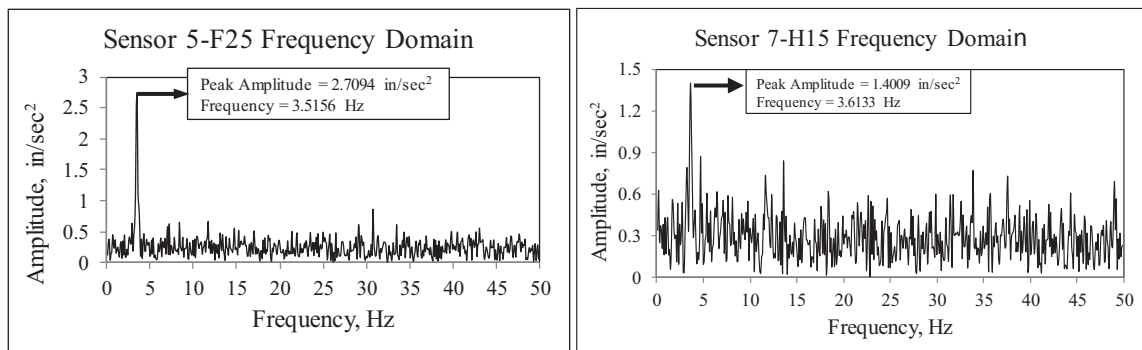


Figure 4.4: Peak amplitude and its corresponding fundamental frequency-Field.

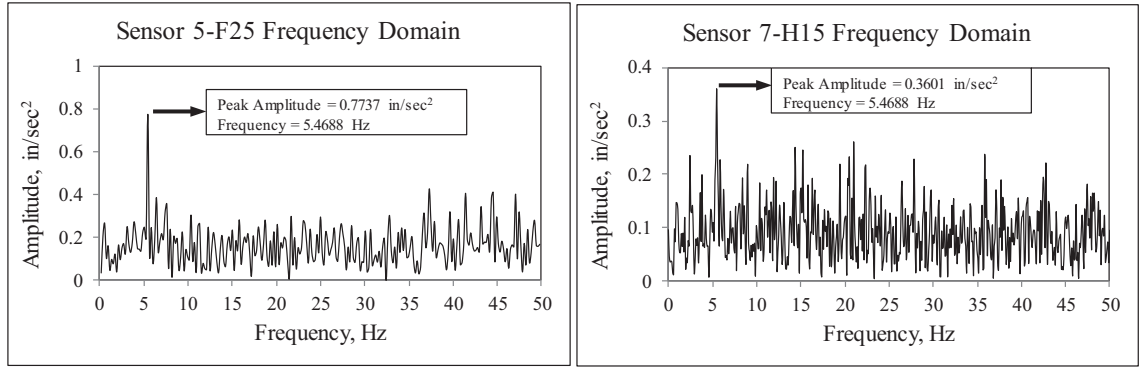


Figure 4.5: Peak amplitude and its corresponding fundamental frequency-FEA.

The peak amplitudes for all the truck runs from the field and the FEA bridge models are shown in Tables 4.2 and 4.3, respectively. The fundamental frequencies corresponding to the peak amplitudes from the field and the FEA bridge models are shown in Tables 4.4 and 4.5, respectively.

Table 4.2: Bridge peak amplitude-Field

Truck	Speed (mph)	Bridge Peak Acceleration Amplitude-Field (in/sec ²)							
		1	2	3	4	5	6	7	8
Empty	10	0.7499	0.5698	0.8015	0.7739	0.8177	0.6032	0.76	0.4036
	15	0.7403	0.8494	0.8672	0.964	0.9174	0.8463	0.7496	1.06
	20	0.604	0.67	0.6731	0.7939	0.718	0.6533	0.4172	1.0856
	25	0.5717	0.6828	0.6269	0.7475	0.5611	0.4449	0.4683	0.536
Half-loaded	10	0.7968	0.5372	1.1876	1.0212	1.1997	0.764	0.7868	0.7979
	15	1.1896	1.3009	1.3067	1.4836	1.5935	1.2862	1.4009	1.0629
	20	1.0671	1.1051	2.2269	1.619	1.6344	1.5373	1.3762	1.4366
	25	0.7756	0.9033	0.7905	0.6671	0.944	0.7674	1.013	0.8163
Fully-loaded	10	0.856	0.5005	0.6876	0.9099	0.5487	0.7202	0.6857	0.4597
	15	1.1336	1.3086	1.2047	1.3405	1.1901	1.3547	1.3529	1.1107
	20	0.8125	0.9708	1.1406	1.0386	1.055	1.1537	1.1223	0.8568
	25	2.1988	2.3635	2.6689	2.2605	2.7094	2.9505	2.5981	1.8354

Table 4.3: Bridge peak amplitude-FEA

Truck	Speed (mph)	Bridge Peak Acceleration Amplitude-Abaqus (in/sec ²)							
		1	2	3	4	5	6	7	8
Empty	10	0.3938	0.2763	0.4914	0.4645	0.4385	0.487	0.2731	0.4472
	15	0.3132	0.3064	0.2361	0.3591	0.4023	0.3767	0.3377	0.2871
	20	0.496	0.6078	0.701	0.6699	0.7919	0.7049	0.5976	0.7733
	25	0.5818	0.4896	0.5979	0.7699	0.9861	0.6733	0.5728	0.4653
Half-loaded	10	0.2798	0.3254	0.342	0.3833	0.4774	0.3154	0.2956	0.3594
	15	0.4349	0.3951	0.404	0.373	0.3919	0.3537	0.3601	0.265
	20	0.6783	0.5045	0.4883	0.7517	0.5461	0.7238	0.5604	0.6152
	25	0.4818	0.5701	0.6864	0.8603	0.7394	0.5213	0.5829	0.6485
Fully-loaded	10	0.373	0.3348	0.3412	0.3697	0.4146	0.4257	0.3822	0.2905
	15	0.492	0.3419	0.4074	0.3349	0.3647	0.2758	0.304	0.3739
	20	0.6706	0.826	0.7616	0.5884	0.7719	0.599	0.713	0.5601
	25	0.6876	0.6921	0.7019	0.925	0.7737	0.8321	0.7175	0.6336

Table 4.4: Bridge fundamental frequency-Field

Truck	Speed (mph)	Bridge Frequency-Field (Hz)							
		1	2	3	4	5	6	7	8
Empty	10	2.9297	3.3203	3.418	4	3.5156	3.5156	3.5156	3.3203
	15	3.6133	3.7109	3.5156	3.5156	3.6133	3.6133	3.6133	3.5156
	20	3.6133	3.418	3.6133	3.418	3.0273	3.2227	3.027	3.2227
	25	3.3203	3.3203	3.3203	3.6133	3.8086	3.3203	3.125	3.0273
Half-loaded	10	3.3203	3.418	3.5156	3.5156	3.418	3.418	3.418	3.5156
	15	3.5156	3.5156	3.5156	3.6133	3.6133	3.5156	3.6133	3.6133
	20	3.418	3.418	3.418	3.418	3.5156	3.418	3.418	3.5156
	25	3.418	3.2227	3.809	3.7109	3.418	3.3203	3.418	3.3203
Fully-loaded	10	3.418	3.418	3.7109	3.418	3.2227	3.125	3.125	3.6133
	15	3.5156	3.418	3.418	3.5156	3.418	3.5156	3.418	3.5156
	20	3.5156	3.5156	3.2227	3.3203	3.3203	3.418	3.125	3.2227
	25	3.418	3.418	3.418	3.5156	3.5156	3.418	3.5156	3.5156

Table 4.5: Bridge fundamental frequency-FEA

Truck	Speed (mph)	Bridge Frequency-Abaqus (Hz)							
		1	2	3	4	5	6	7	8
Empty	10	5.5664	5.4688	5.4688	5.3711	5.3711	5.4688	5.3711	5.3711
	15	5.4688	5.3711	5.3711	5.3711	5.4688	5.3711	5.4688	5.3711
	20	5.4688	5.4688	5.4688	5.4688	5.4688	5.4688	5.4688	5.4688
	25	5.4688	5.4688	5.4688	5.4688	5.4688	5.4688	5.4688	5.4688
Half-loaded	10	5.4688	5.3711	5.3711	5.3711	5.4688	5.3711	5.4688	5.3711
	15	5.4688	5.3711	5.4688	5.3711	5.4688	5.4688	5.4688	5.4688
	20	5.4688	5.4688	5.4688	5.4688	5.4688	5.4688	5.4688	5.4688
	25	5.4688	5.4688	5.4688	5.4688	5.4688	5.4688	5.4688	5.4688
Fully-loaded	10	5.3711	5.3711	5.566	5.3711	5.4688	5.3711	5.4688	5.3711
	15	5.4688	5.4688	5.4688	5.3711	5.3711	5.4688	5.3711	5.4688
	20	5.4688	5.4688	5.4688	5.4688	5.4688	5.4688	5.4688	5.4688
	25	5.4688	5.4688	5.4688	5.4688	5.4688	5.4688	5.4688	5.4688

4.5 MAC Analysis of Field and Model Data

The modal analysis between each sensor location of both the new (FEA bridge model) and old bridge (bridge at the current condition) under different loads and speeds was carried out by using the modal assurance criterion (MAC) analysis. The MAC analysis of peak amplitudes indicates the degree of correlation or linearity between each set of data from the field and the FE model. The MAC value for each pair of similar sensors is calculated by Eq. 4.6.

$$MACn = \frac{(N_n^T \cdot O_n^T)^2}{(N_n^T \cdot N_n) * (O_n^T \cdot O_n)} \quad (4.6)$$

Where,

$MACn$ = MAC value for the n^{th} sensor nodes.

N_n = Amplitude response matrix of the n^{th} sensor of the FE bridge model

O_n = Amplitude response matrix of the n^{th} sensor of the existing bridge.

N_n^T = Transpose of the amplitude response matrix of N_n .

O_n^T = Transpose of the amplitude response matrix of O_n .

The illustration of the MAC calculations for Sensors 1 and 4 are shown in Appendix C. The MAC values for all sensors are calculated the same way and shown in Table 4.6.

Table 4.6: Sensors with corresponding MAC values

Sensors	MAC Value
1	0.866
2	0.819
3	0.752
4	0.817
5	0.718
6	0.778
7	0.789
8	0.851

4.6 Results

The overall dynamic response of the bridge was tested under different load scenarios. The acceleration data were collected on the bridge at eight sensor nodes, which represented the response of the entire bridge. It is clear from the field and the FEA graphs and tables that there are distinct differences between the response of the bridge at its

newest (FEA models) and current (field) condition. As a bridge ages, damage and deterioration in terms of loss in cross-section, material degradation, corrosion of steel, etc., cause decrease in the stiffness or the flexural rigidity of the bridge. From the theory of structural dynamics, the natural frequency of a structure is directly proportional to the square root of the stiffness or the flexural rigidity. It was noticed from the results that the fundamental frequency of the bridge at its current condition was less than the fundamental frequency at its newest condition, while the amplitude was higher in the current bridge than that in the new bridge. Therefore, the change in fundamental frequency indicates structural damage and deterioration in the bridge over its life time. The reduction or change in fundamental frequency in the bridge between its newest and existing conditions is calculated and linked to the current condition rating of the existing bridge between “zero” (failed condition) and “nine” (excellent condition), which is used by the ODOT and other state DOTs. The descriptions for each of these numeric values are shown in Table 4.7 (FHWA, 2011).

Table 4.7: National Bridge Inventory General Condition Rating Guidance

Code	Description	Commonly Employed Feasible Actions
9	EXCELLENT CONDITION.	Preventive Maintenance
8	VERY GOOD CONDITION No problems noted.	
7	GOOD CONDITION Some minor problems.	
6	SATISFACTORY CONDITION Structural elements show some minor deterioration.	Preventive Maintenance; and/or Repairs
5	FAIR CONDITION Primary structural elements are sound but may have some minor section loss, cracking, spalling or scour.	
4	POOR CONDITION Advanced section loss, deterioration, spalling or scour.	Rehabilitation or Replacement
3	SERIOUS CONDITION Loss of section, deterioration spalling or scour have seriously affected primary structural components. Local failures are possible. Fatigue cracks in steel or shear cracks in concrete may be present.	
2	CRITICAL CONDITION Advanced deterioration of primary structural elements. Fatigue cracks in steel or shear cracks in concrete may be present or scour may have removed substructure support. Unless closely monitored, the bridge may have to be dosed until corrective action is taken.	
1	IMMINENT FAILURE CONDITION Major deterioration or section loss present in critical structural components or obvious vertical or horizontal movement affecting structure stability. Bridge is closed to traffic but corrective action may put back in light service.	
0	FAILED CONDITION Out of service - beyond corrective action.	

From Tables 4.4 and 4.5, it was found that the change in the fundamental frequency of the bridge between sensor locations is fairly small. However, the goal of this study is to estimate the overall structural condition of the bridge rather the condition at a specific location. Therefore, the average of the fundamental frequencies at all sensor locations under various load cases is used in calculating the change in frequency.

From Table 4.4, the average fundamental frequency of the bridge at the current condition (field) is 3.4383 Hz. From Table 4.5, the average fundamental frequency of the bridge at the newest condition (FEA bridge model) is 5.4464 Hz. The reduction in fundamental frequency of the bridge was calculated and it was 36.87%. The detail calculations are shown in Appendix C.

The current condition rating of the bridge is already performed by ODOT and the bridge is given a rating of 6 on the 0-9 numerical scale. This rating means that the bridge health has declined by 3 numeric values due to damage and deterioration over its 25 years of service life. The reduction in frequency of the bridge is linked to the current condition rating of 6 given by ODOT. This relationship is then used to develop the application software algorithms, which can be used to determine the current condition rating of a single span PSBB bridge.

4.7 Application Software Algorithms

In order to estimate the current condition of a bridge, two fundamental frequencies are required to calculate the percent of reduction in fundamental frequency: one from the current condition of the bridge, and the other one from the newest condition of the bridge. The current fundamental frequency can be obtained from the field acceleration data captured through WSN. The fundamental frequency at the newest condition can be determined using two methods: FE simulation and theory of structural dynamics. Since the application software developed in this study is aimed to instantly estimate the current condition rating of a bridge, the use of FE simulation in the field is not practical. Therefore, the theory of structural dynamics is used to determine the fundamental

frequency of a bridge at its newest condition. However, the FEA was used in this study to find the fundamental frequency of the Ashtabula Bridge at its newest condition by creating FE models that closely represented the bridge at its newest condition. Therefore, the fundamental frequency found by the theory of structural dynamics needs to be corrected for its corresponding fundamental frequency in FEA. For the algorithms of the application software, a relationship between both FEA and theory of structural dynamics is calculated in determining the fundamental frequency of the Ashtabula Bridge at its newest condition.

The fundamental frequency of the bridge at its newest condition can be found from the theory of structural dynamics by using the equations in Table 4.1. For a beam with fixed-fixed support condition, the fundamental frequency calculations are performed by using Eqs. 4.7 to 4.9.

$$f = 3.5608 * \sqrt{\frac{EI}{mL^4}} \quad (4.7)$$

Let: $mL = m_t$ (4.8)

Where, m_t = total mass of the beam.

Then Eq. 4.7 can be re-written as Eq. 4.9.

$$f = 3.5608 * \sqrt{\frac{EI}{m_t L^3}} \quad (4.9)$$

In the above equations, the fundamental frequency is a function of total mass, flexural rigidity, and length of the bridge. The total mass of the bridge does not change significantly over time. Therefore, it was assumed constant and found from the FE model

simulation output. The total mass of the bridge: $m_t = 2193.1 \frac{lb.s^2}{in}$, and the length of the PSBB: $L = 1020 in$.

The flexural rigidity, EI , of the bridge can be determined from its geometry and material properties. According to ACI Building Code Section 8.5.1 (ACI, 2008), the modulus of elasticity, E_c , of concrete can be calculated by Eq. 4.10.

$$E_c = 33 w_c^{1.5} \sqrt{f'_c} \quad (4.10)$$

Where, E_c = modulus of elasticity of concrete in (psi), w_c = unit weight of concrete in (lb/ft³), f'_c = 28-day compressive strength of concrete in (psi).

From the ODOT bridge design data, the unit weight of concrete of the box beams was 150 lb/ft³, and the 28-day compressive strength was 5,500 psi. Substituting these values in Eq. 4.10 produces: $E_c = 4,496,061 psi$.

The moment of Inertia, I , of the box beams was found by Eq. 4.11.

$$I = \left(\frac{W_o H_o^3}{12} - \frac{W_i H_i^3}{12} \right) * n_b \quad (4.11)$$

Where,

W_o : Box Beam Outside Width (in.)

H_o : Box Beam Outside Height (in.)

W_i : Box Beam Inside Width (in.)

H_i : Box Beam Inside Height (in.)

n_b : Number of Box Beams.

The moment of inertia was calculated and equal to: $I = 1,776,376 in^4$.

Now, the fundamental frequency of the bridge can be calculated by using Eq. 4.9, and it gives: $f = 6.5963 \text{ Hz}$.

The difference between the fundamental frequencies of the bridge found by FEA and theory, Δf_{new} , is calculated as $\Delta f_{\text{new}} = 0.174$. The detail calculations are shown in Appendix C. This 0.174 difference in frequency was expected, and it shows that the theoretical method produces higher frequency values than the FE method. Therefore, multiplying the theoretical frequency by $(1 - 0.174)$ or 0.826 produces the frequency in the FE method.

The 36.87 % frequency decrease was equivalent to 3 unit rating decrease on the 0-9 NBI numerical scale and produces a 12.29% decrease in frequency for each unit of rating.

The reduction in the health of the bridge, G , is expressed by Eq. 4.12.

$$G = \Delta f * \frac{10000}{1229} \quad (4.12)$$

The current condition rating of the bridge is calculated by Eq. 4.13.

$$\text{Bridge Condition Rating} = \text{integer}(9 - G) \quad (4.13)$$

Figures 4.6 to 4.8 show the algorithms for the application software and the procedures for bridge condition assessment developed in this study. Figure 4.9 shows schematic diagrams of bridge geometric parameters used in the flow chart.

Input:

1. L: Box Beam (PSBB) Length (in)
2. W_o : Box Beam Outside Width (in)
3. W_i : Box Beam Inside Width (in)
4. H_o : Box Beam Outside Height (in)
5. H_i : Box Beam Inside Height (in)
6. n_b : Number of Box Beams
7. n_d : Number of Diaphragms per Box Beam
8. t_d : Thickness of Diaphragms (in)
9. t_c : Thickness of Box Beam ends (in)
10. t_w : Thickness of Asphalt Concrete Wearing Surface (in)
11. f'_c : 28-day Compressive Strength of Concrete (psi)
12. w_c : Unit Weight of Concrete (lb/ft³)
13. Bridge End Supports. (Drop Down menu)
 - a) Fixed-Fixed
 - b) Fixed-Hinged
 - c) Simply Supported

Figure 4.6: Bridge condition assessment input page.

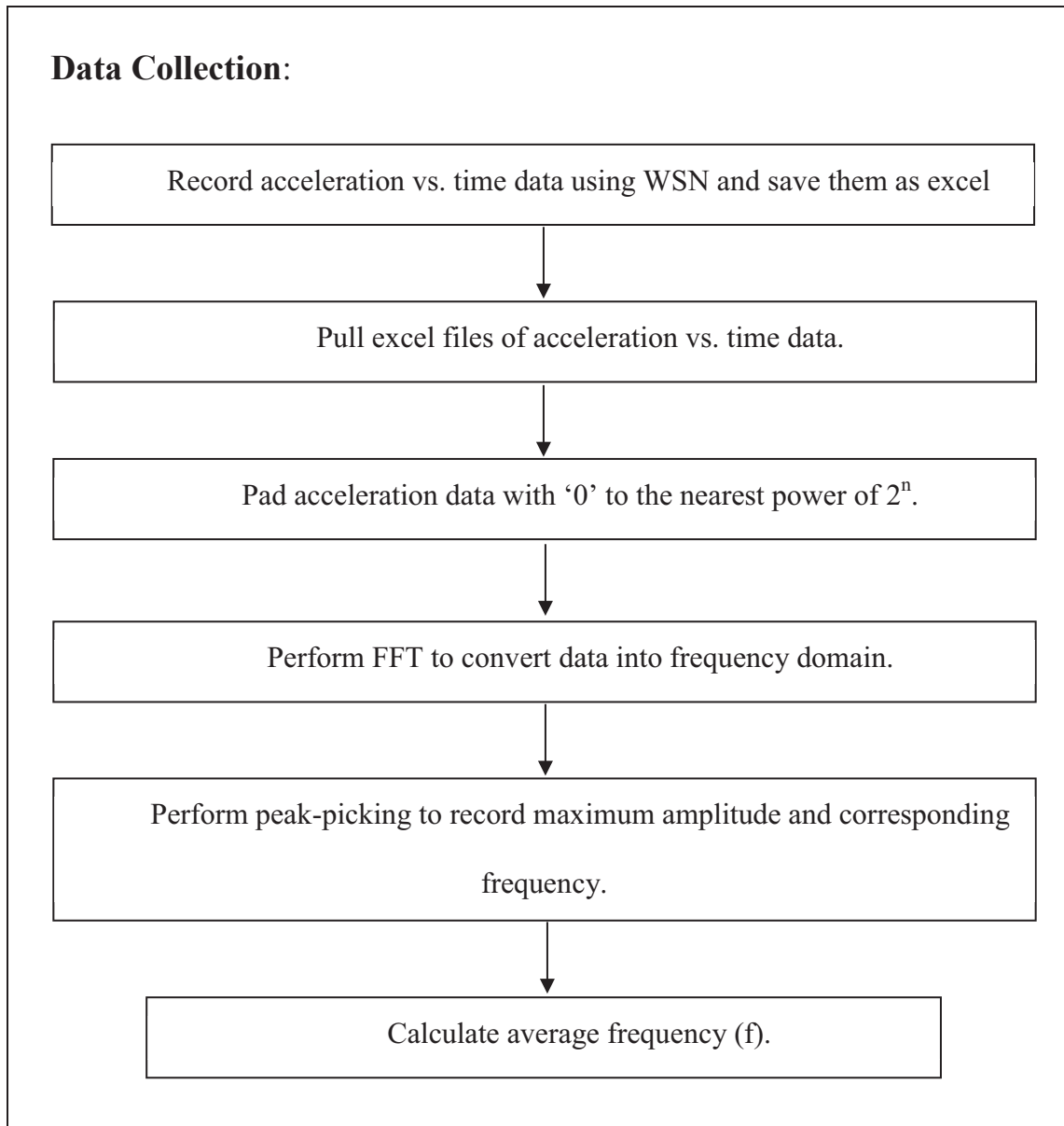


Figure 4.7: Bridge condition assessment flow chart.

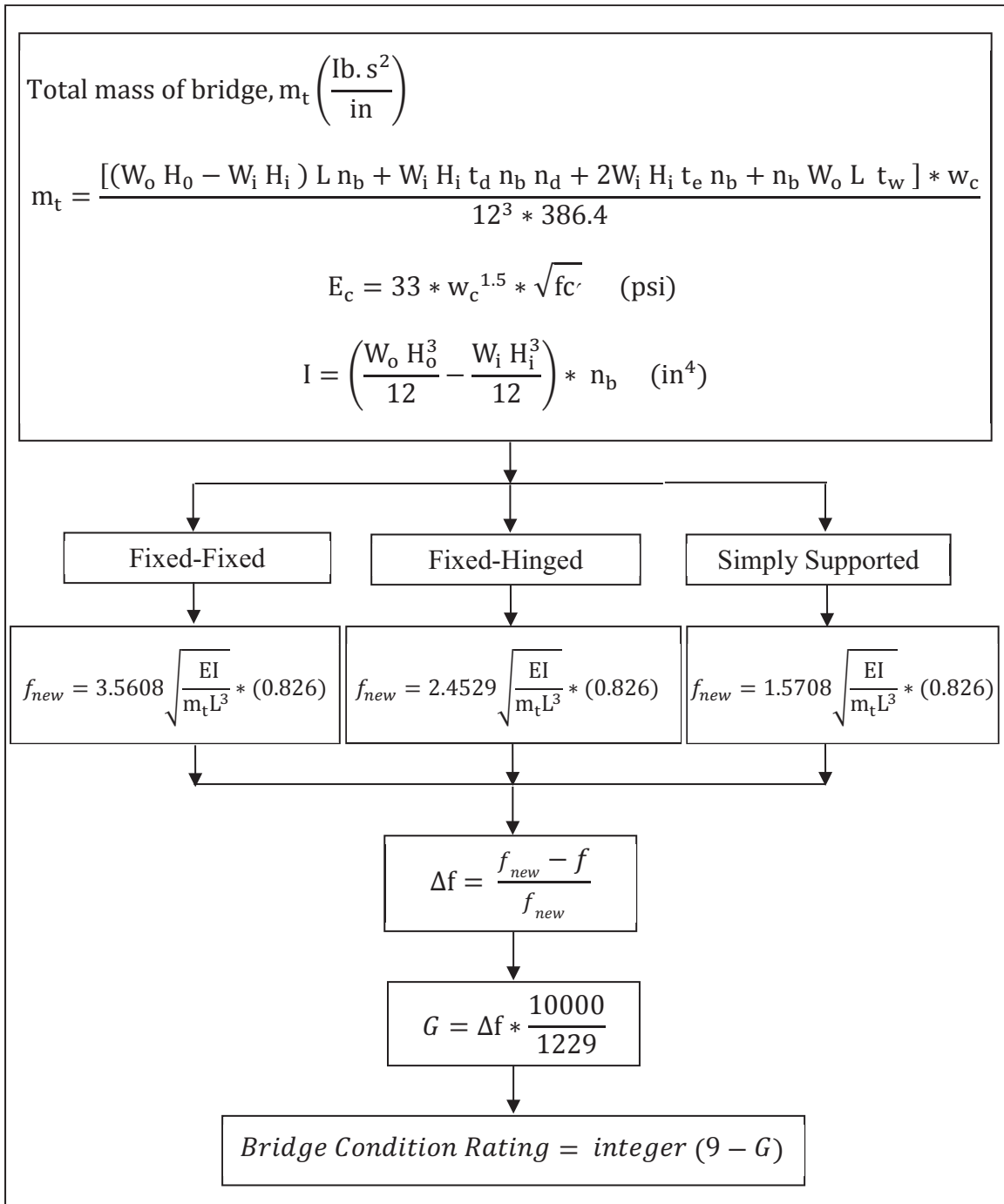


Figure 4.8: Bridge condition assessment flow chart (continued).

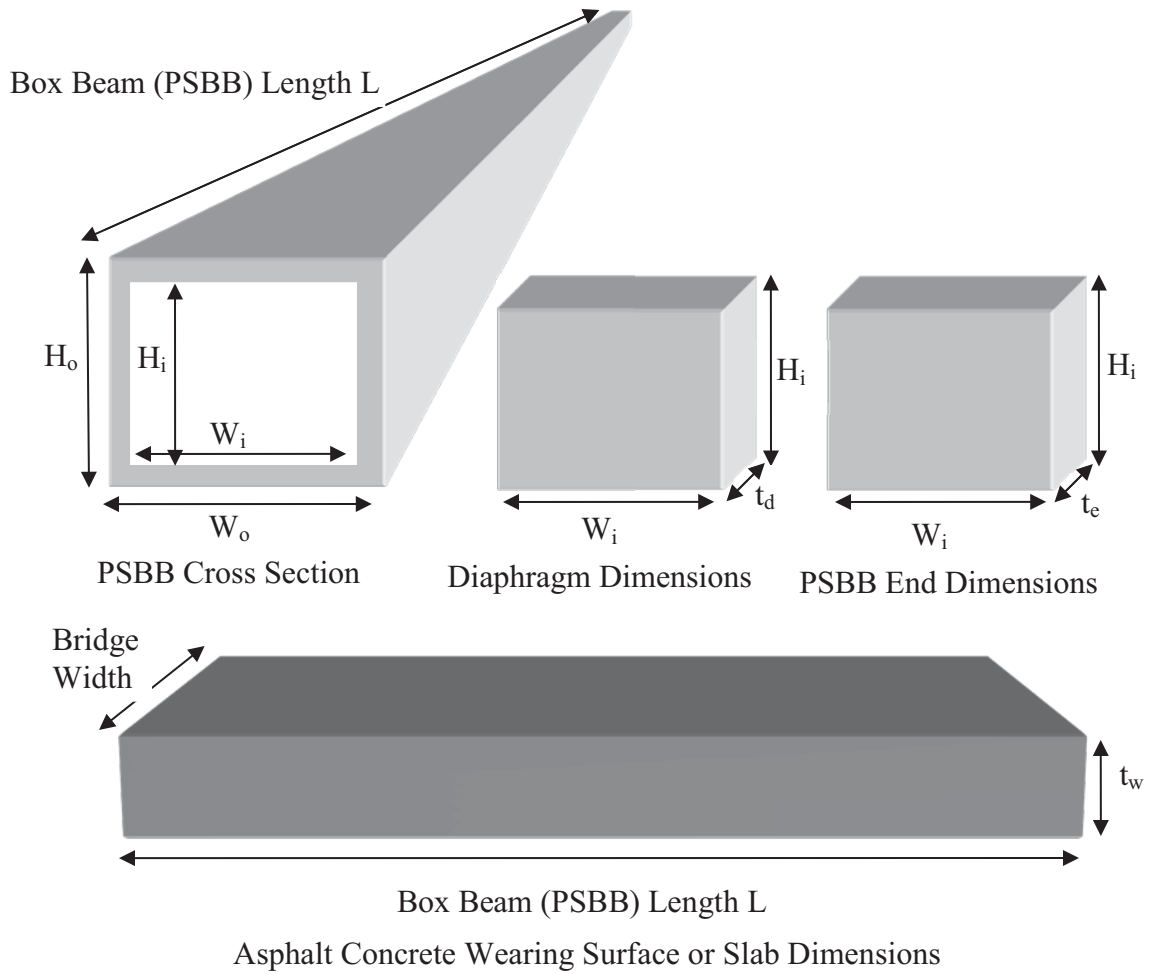


Figure 4.9: PSBB bridge geometric property.

4.8 FE Model Validation

The essential task in finite element modeling and analysis is to check that the finite element model assumed to represent a real structure is mathematically correct. Therefore, it is necessary to validate the FE model to ensure the reliability and accuracy of the results. The FE model in this study was validated using two methods: (1) experimental validation by using frequency analysis and (2) theoretical validation by using static analysis.

4.8.1 Experimental Validation

The modulus of elasticity (MOE) of concrete is a variable that plays important role in the dynamic bridge response. It is the primary material property of the bridge in the FE simulation. The MOE of the bridge at the current condition was calculated. The detail calculations are shown in Appendix C. An FE model, which represented the bridge at its current condition, was created for the bridge based on the current MOE, and the frequency analysis was performed to extract the fundamental frequency of the bridge.

From the results of the FEA, the fundamental frequency, as shown in Fig. 4.10, was equal to 3.5505 Hz. This result was very close to the experimental fundamental frequency of 3.4383 Hz of the bridge at current condition obtained from the analysis of the acceleration data collected in the field.

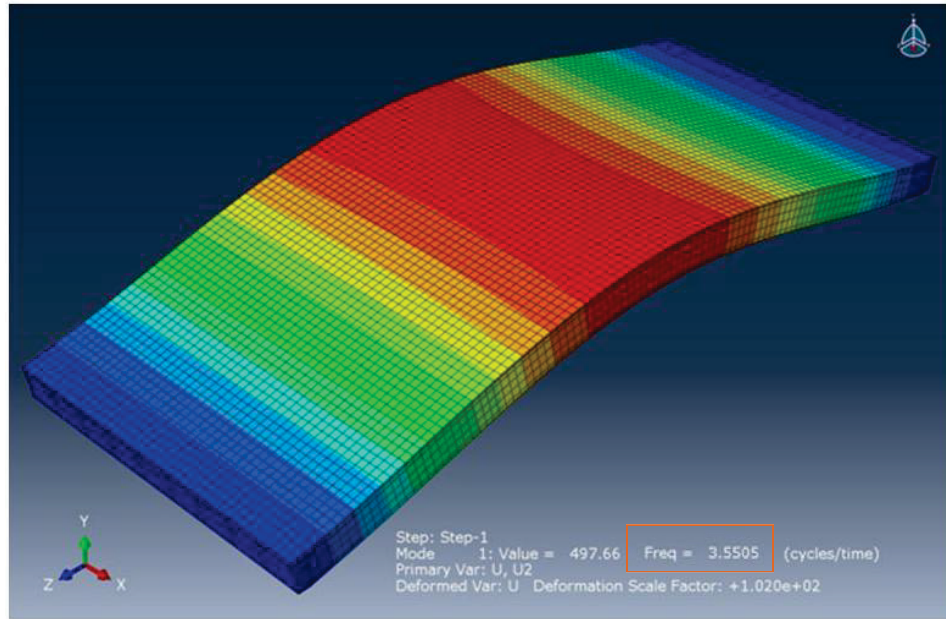
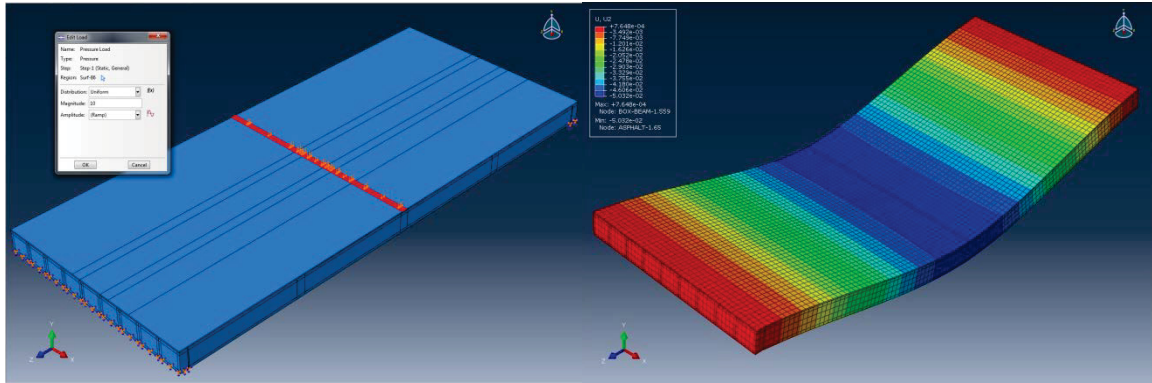


Figure 4.10: Fundamental frequency of Ashtabula Bridge at current condition.

4.8.2 Theoretical Validation

A static pressure of 10 psi was applied through a 12 in. wide and 432 in. long strip across the bridge, as shown in Fig. 4.11. The pressure was applied at the middle of the bridge so that its effect is uniformly distributed. A static analysis was performed in FE, and the values for the maximum stress, the maximum deflection and the total mass of the bridge were obtained from the FE output. On the other hand, the theoretical hand calculations were carried out to find the maximum stress, the maximum deflection and the total mass of the bridge under the same loading condition, and the results were compared to those that were obtained from the FEA. The detail calculations are shown in Appendix C.



(a)

(b)

Figure 4.11: FE model validation: a) pressure, b) deflected shape (exaggerated).

The summary of the results from the FEA and the theoretical hand calculation is shown in Table 4.8.

Table 4.8: Comparison of results from FEA and approximate calculations

Items	FEA	Hand Calculations
Maximum stress	73 psi	78.14 psi
Maximum deflection	0.05 in.	0.036 in.
Total mass	2193.1 lb.s ² /in	2154.321 lb.s ² /in
Fundamental frequency	3.5505 Hz	3.4383 Hz*

Note: * means the value is found from FFT and peak-picking method.

As it can be seen from Table 4.8, the results from both the FEA and the approximate hand calculations are fairly close. In view of the above analyses and comparisons, it can be concluded that the FEA bridge model very closely represents the bridge at its newest condition.

4.9 Application Software and Verification

The application software, called “ODOTApp”, was developed on Microsoft’s .NET4.5 framework based on the research outcomes and the flow chart, as shown in Figs. 4.6 to 4.8. This software requires inputs for bridge geometric, materials and support conditions, truck parameters and dynamic response of a PSBB bridge under a heavily loaded truck at two different speeds, such as 10 and 25 mph. Figures 4.12 and 4.13 show the “Input Parameters” and “Bridge Assessment” tabs, respectively, of the application software using dynamic response data of Ashtabula Bridge.

The screenshot displays the 'Input Parameters' tab of the 'Bridge Condition Assessment and Load Rating' application. The interface is organized into several sections:

- Box Beam:** A list of input fields with values: PSBB Length (in.) = 1020, Outside Width (in.) = 48, Inside Width (in.) = 38, Outside Height (in.) = 42, Inside Height (in.) = 31.5, Number of Box Beams = 9, Number of Diaphragms / Box Beam = 3, Diaphragm Thickness (in.) = 18, and Box Beam End Thickness (in.) = 18.
- Concrete:** Input fields for 28-day Compressive Strength (psi) = 5500 and Unit Weight (pcf) = 150.
- Bridge:** Radio buttons for Pedestrian sidewalks (Yes/No), a dropdown for End Supports (Fixed-Fixed), and an input field for Wearing Surface Thickness (in.) = 2.5.
- Truck:** A section for Truck #1 with input fields for Weight (lb) = 32300, Speed #1 (mph) = 10, and Speed #2 (mph) = 25.

At the bottom right, there is a prominent 'Load Sensor Data' button and a status message 'Sensor Data Loaded!'.

Figure 4.12: Input Parameters tab of ODOTApp with loaded dynamic response data.

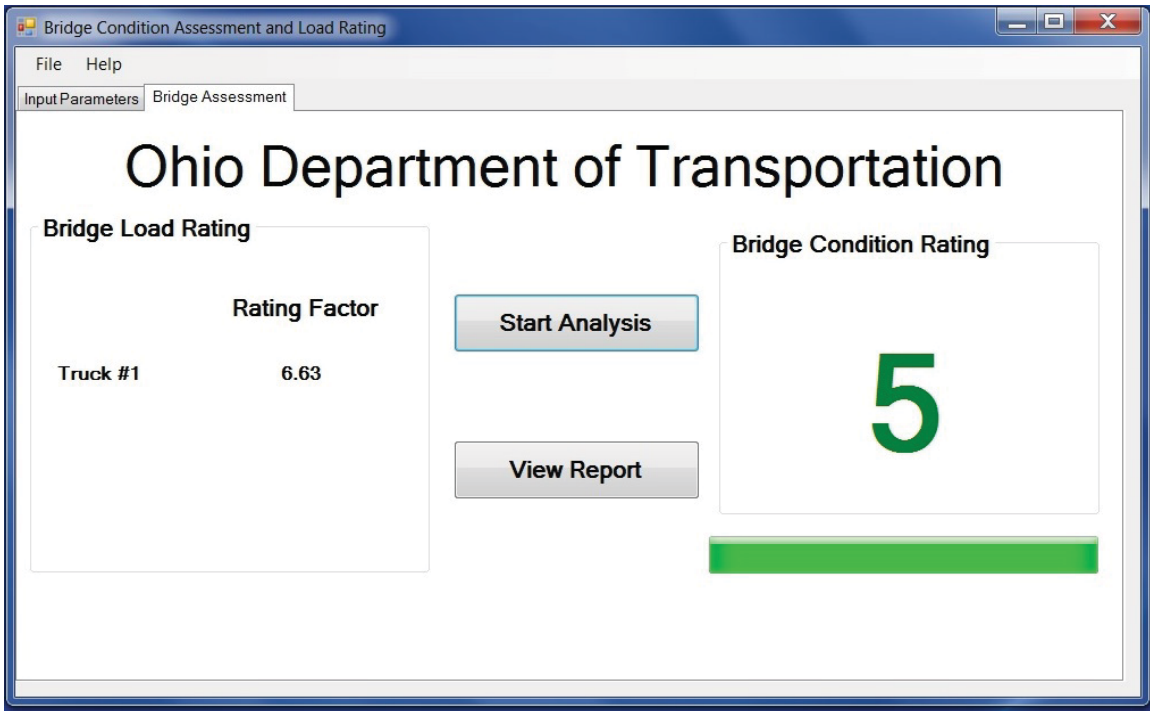


Figure 4.13: Bridge Assessment tab of ODOTApp after analysis.

The input parameters are self-explanatory. Usually, these data are available from the bridge design and construction plans. The “Load Sensor Data” requires selecting the files of bridge dynamic response. The sensor data, which are acceleration data of a bridge, must be loaded before going to the Bridge Assessment tab and run the analysis.

The Bridge Assessment tab has two buttons, Start Analysis and View Report, as shown in Fig. 4.13. The analysis can be started by clicking the Start Analysis button, and the results of the analysis will be shown in both the Bridge Load Rating and Bridge Condition Rating dialog boxes. The analysis report, which contains tables and results of the analysis, can be viewed by clicking the View Report button. The analysis of the data collected on Ashtabula Bridge using the application software produced the following results: Bridge Load Rating (Rating Factor) of 6.63 based on the truck weight, and Bridge

Condition Rating of 5 based on a scale of 0-9. These results are close to ODOT's rating. It should be noted herein that this research performed bridge condition rating while another research was performed simultaneously to estimate the bridge load rating. The application software was developed by combining the results and algorithms from both studies. In this way, the application software as combined herein will be more cost-effective since both condition rating and load rating of a PSBB bridge can be performed simultaneously using its dynamic response collected under a heavily loaded truck at two different speeds.

In order to check if the methodology proposed and followed in this research was working realistically, and to make sure the codes and formulas used in developing the software were accurate, it was very important to verify the ODOTApp application software in the field. For this purpose, the dynamic response data of a Trumbull County Bridge TRU-45.1699 (Trumbull Bridge) under a 43,100 lb truck (data shown in Appendix A) at 10 and 25 mph were collected using the same procedure used during data collection on Ashtabula Bridge. After changing the names of the acceleration data files, the ODOTApp was run on site to estimate the load and condition rating of the bridge. Figures 4.14 and 4.15 show the input and output tabs, respectively, using dynamic response of Trumbull Bridge in Trumbull County, Ohio.

The input data were collected from the bridge design and construction plans provided by ODOT, and the truck parameters were collected on site. Once the analysis was performed, the output tab shows a load rating factor of 13.69 and a condition rating of 8, which are close to ODOT's ratings. After on-site validation, the researchers believe

that the application software can be used to instantly estimate the load and condition ratings of a PSBB bridge on site.

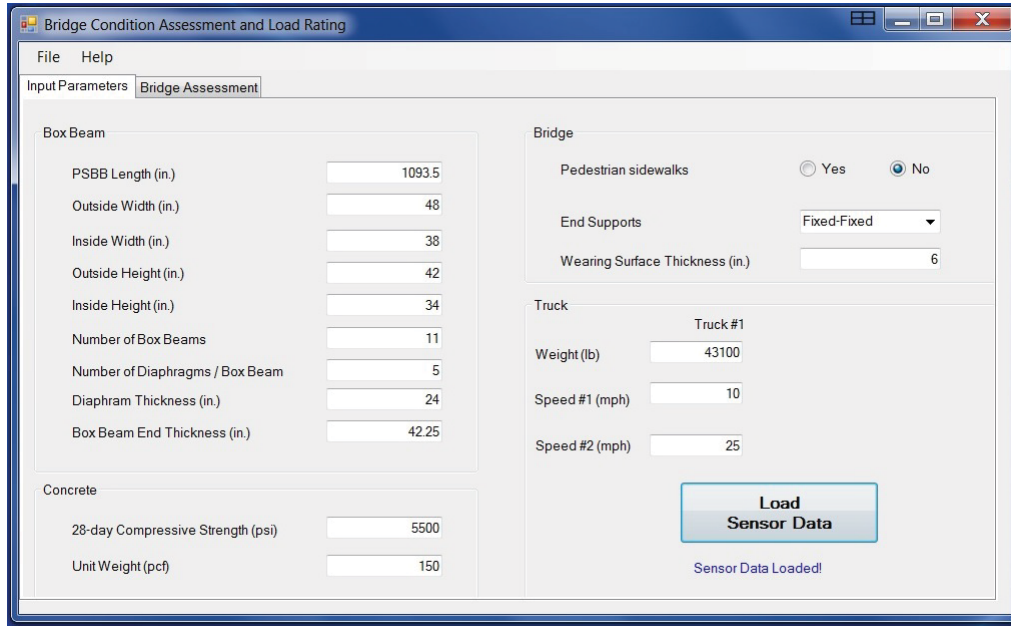


Figure 4.14: Input Parameters tab of ODOTApp with Trumbull Bridge response.

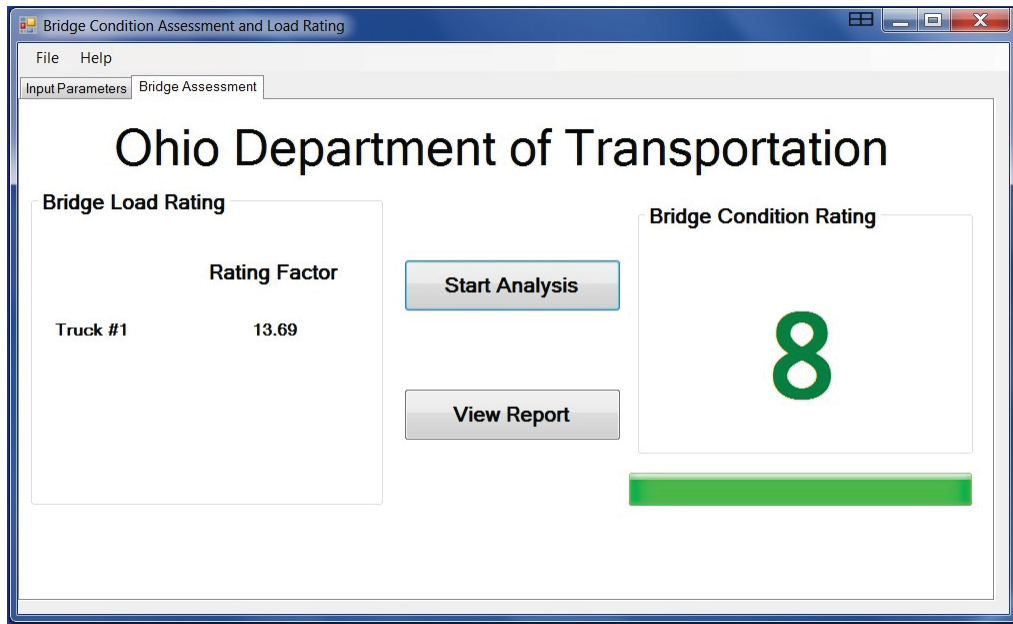


Figure 4.15: Output tab of ODOTApp with Trumbull Bridge response.

4.10 Discussions

The objective of this research was to develop a tool for condition assessment of a PSBB bridge under vehicular loads by analyzing its dynamic response collected through WSN. The stated objective was achieved through the analyses of the collected dynamic response data and determining the relationship between the response data of the bridge at its newest and current conditions. The hypothesis is based on the assumption that the dynamic response is a sensitive and important indicator of the physical integrity and condition of a structure. The following findings are summarized from the outcome of this study:

- After 25 years in service, the frequency of the bridge has decreased by 36.87%. This change in frequency was correlated to the current condition rating of the bridge performed by ODOT. The bridge was given a rating of 6 on the numerical scale of 0-9 of NBI. The description of this rating by NBI is "Satisfactory Condition, Structural elements show some minor deterioration". Those bridges are usually designed and built to last around 50 years. However, the bridge still has sufficient capacity for supporting current traffics. Therefore, the 36.87% decrease in frequency after 25 years of service is expected, practical and reasonable.
- The values of MAC analysis vary along the length of the bridge. The sensors, which are closer to the bridge ends, produce higher MAC values than those close to the middle of the bridge. The average MAC value was 0.799, which estimates the degree of correlation between the field and FE bridge model data. In practice,

MAC values greater than 0.9 are considered as well correlated sets of data (Ewins, 2000).

- From the fundamental frequency Tables 4.4 and 4.5 from the field and the FEA models, respectively, it can be noticed that the fundamental frequency was not significantly affected by the changes in weight and speed of the trucks. This is acceptable because the weights of the trucks were very small compare to the weight of the bridge itself. Therefore, in the modal analysis of the bridge using the theory of beam systems, the mass of the trucks did not affect the calculations of the fundamental frequency. On the other hand, the amplitudes of the bridge, as shown in Tables 4.2 and 4.3, were greatly affected by the changes in weights and speeds of the trucks.
- From the tables of fundamental frequencies and peak amplitudes, it can be found that the frequency of the bridge at the current condition is less than its frequency at the newest condition, while the amplitude of the bridge at the current condition is higher than its amplitude at the newest condition. These results agree with the fact that a bridge ages and deteriorates over time, and its frequency decreases while its amplitude increases under the same loading condition.

Chapter 5

Conclusions and Recommendations

5.1 Conclusions

The role of health monitoring is vital to ensure public safety by detecting structural damage and deterioration of a bridge from its dynamic response under vehicular loads. In bridge engineering, the concept of health monitoring is widely applied to assess structural integrity of bridges, and to maintain their safe and continuous operation. The method described in this study and the application software developed from the data analysis provide an efficient and cost-effective solution for assessing the overall condition of a PSBB bridge. The concept used in this study of bridge condition assessment is based on the hypothesis that the dynamic structural response of a new bridge under vehicular loads will be quite different than that of the same bridge after, say, 20 years, due to the deterioration of the bridge over time. Therefore this difference, which estimates the amount and average rate of bridge deterioration, can be assessed by analyzing the dynamic structural response of a bridge at its newest and existing conditions.

The outline of the methodology used in this study can be summarized in the following steps:

- Collecting acceleration vs. time data of a PSBB bridge under vehicular loads through a system of wireless sensor networks in the field.

- Developing a full-scale 3D bridge model using ABAQUS to represent the bridge at its newest condition, and analyzing the FE models to obtain acceleration vs. time data.
- Performing FFT to transform collected time data into frequency domain for further analysis.
- Performing peak-picking method to record maximum amplitude and its corresponding fundamental frequency.
- Analyzing the data from both field and FE bridge models to assess the overall structural condition of the bridge.

From the results of the data analysis, it was observed that the values of MAC analysis change along the length of the bridge, and it gives higher values at the points closer to the end supports and it decreases as it gets closer to the middle of the bridge. Also, it is shown that the fundamental frequency of the bridge has decreased while its amplitude has increased over the 25-year service life of the bridge. The reduction in the fundamental frequency over 25 years of service is 36.87%, and this reduction is correlated to the current general condition rating of 6 performed by the Ohio Department of Transportation.

The fundamental frequency of the bridge at its newest condition is also calculated using the theoretical method, and it is compared with the fundamental frequency found from the FEA bridge models. A relationship between these frequencies was established. The 36.87% reduction in frequency is used in developing the algorithm for the bridge condition rating application software. In this algorithm, the structural condition of a PSBB bridge is assessed from the reduction in the fundamental frequency between its

newest and existing conditions. The fundamental frequency of a bridge at the current condition is found from its dynamic response, while the fundamental frequency of the same bridge at its newest condition is calculated from its geometric and material properties. The reduction in frequency is then correlated to the standard general condition ratings of bridges established by the National Bridge Inventory to assess the structural condition of a bridge. The application software will in no way replace the existing methods of bridge condition rating, but may be used simultaneously to develop a database of the dynamic response of various bridges. This database will be very important and useful for incorporating into the application software to make it more robust, acceptable and effective.

5.2 Recommendations

In light of the outcome of this research, some possible areas of future work have been identified and described below.

- The primary focus of this research was on prestressed concrete box beam bridges. Therefore, it is suggested that future work be performed on various bridge types, such as truss, steel, and long span bridges.
- The effect of structural damage on the higher frequency modes should be further investigated.
- Further studies are recommended to determine the relation of MAC analysis with the amount and location of damage.
- Defining interaction forces between the vehicle and bridge in the finite element analysis including roughness of bridge deck may improve the outcome.

- Defining the property of bearing pads in the finite element analysis and studying their effect on dynamic response of bridges may also be included.
- Dynamic response of bridges can also be further investigated under the effect of multiple moving trucks.
- If more bridges can be tested, a more precise relationship can be obtained from the comprehensive analysis of all the collected dynamic bridge response data.

References

1. American Society of Civil Engineers (ASCE, 2013). “Report Card on America’s Infrastructure”, 1801 Alexander Bell Drive, Reston, Virginia.
2. Lynch, J. P. (2005). “Design of a wireless active sensing unit for localized structural health monitoring”, *Structural Control and Health Monitoring*, Wiley InterScience, 12:405-423.
3. Federal Highway Administration (FHWA, 2004). “Status of the Nation’s Highways, Bridges, and Transit: 2004 Conditions and Performance”. URL: <http://www.fhwa.dot.gov/policy/2004cpr/chap3c.htm#body> as of 10/26/2013.
4. U. S. Department of Transportation (USDOT, 2010). “Transportation Statistics Annual Report”, Bureau of Transportation Statistics.
5. American Association of State Highway and Transportation Officials (AASHTO, 2008). “Bridging the Gap.”
6. National Surface Transportation Policy and Revenue Study Commission (NTSP, 2007). “Transportation for Tomorrow”, Final report, Volume II, Chapter 4, pp. 6.
7. Federal Highway Administration (FHWA, 2004). “NBIS Regulations”, *Rules and Regulations*. Vol. 69, No. 239.
8. Lynch, J. P., Wang, Y., Loh, K. J., Yi, J., and Yun, C. (2006). “Performance monitoring of the Geumdang Bridge using a dense network of high-resolution wireless sensors”, *Smart Materials and Structures*, Vol. 15, pp. 1561-1575.
9. Samali, B., Crews, K., Li, J., Bakoss, S., and Champion, C. (2003). “Assessing the Load Carrying Capacity of Timber Bridges using Dynamic Methods”, Institute of Public Works Engineering Australia, Sydney, NSW, Australia.

10. Federal Highway Administration (FHWA, 2005). "Dynamic Bridge Substructure Evaluation and Monitoring", Publication No. FHWA-RD-03-089.
11. Straser, E. G. and Kiremidjian, A. S. (1998). "A modular, wireless damage monitoring system for structures", John A. Blume Center Technical Report No. 128, Stanford University, Stanford, CA.
12. Doebling, S.,W., Farrar, C. R., Prime, M. B., and Shevitz, D. W. (1996). "Damage Identification and Health Monitoring of Structural and Mechanical Systems from Changes in their Vibration Characteristics: A Literature Review", Report No. LA-13070-MS, Los Alamos National Laboratory. Los Alamos, NM.
13. Kim, S., Pakzad, S., Culler, D., Demmel, J., Fenves, G., Glaser, S., and Turon, M. (2007). "Health Monitoring of Civil Infrastructures Using Wireless Sensor Networks", Proceedings of the 6th International Conference on Information Processing in Sensor Networks (IPSN 2007), Cambridge, MA, ACM Press, pp. 254-263.
14. Gangone, M. V, Whelan, M. J., Janoyan, K. D., and Jha, R. (2008). "Field deployment of a dense wireless sensor network for condition assessment of a bridge superstructure", SPIE Smart Structures Symposium, San Diego, California, 2008.
15. Allemang, R. J. and Brown, D. L. (1982). "A correlation coefficient for modal vector analysis", Proceedings of the 1st International Modal Analysis Conference, Kissimmee, FL. Vol. 1, pp. 110-116.


16. Allemang, R. J. (2002). The Modal Assurance Criterion (MAC): “Twenty Years of Use and Abuse”, Proceedings, International Modal Analysis Conference, pp. 397-405, 2002. Sound and Vibration Magazine, Vol. 37, No. 8, pp. 14-23.
17. Marwala, T. (2010). “Finite-element-model Updating Using Computational Intelligence Techniques”, Applications to Structural Dynamics, Library of Congress Control Number: 2010929648, ISBN 978-1-84996-322-0. DOI 10.1007/978-1-84996-323-7.
18. National Cooperative Highway Research Program (NCHRP, 2009). “NCHRP Synthesis 393, Adjacent Precast Concrete Box Beam Bridges: Connection Details”, Project 20-5 (Topic 39-10), Library of Congress Control No. 2009900728, ISSN 0547-5570. ISBN 978-0-309-098304.
19. Federal Highway Administration (FHWA, 2012). “National Bridge Inventory, Inspection and Evaluation, Bridges By Structure Type, URL: [<http://www.fhwa.dot.gov/bridge/struct.cfm>] as of 10/26/2013.
20. Bridge Design Manual (BDM, 2011). Ohio Department of Transportation, Columbus, Ohio.
21. Prestressed Concrete Institute (PCI, 2009). “The State of the Art of Precast/Prestressed Box Beam Bridges”, Chicago, URL: <http://structureshandouts.unomaha.edu/Precast%20deck%20110825/Archive/NUDECK/PCI%20Adjacent%20Box%20Beam%20Bridges%204-21-09.pdf> as of 10/26/2013.
22. Google Maps (2013). [MAH-45-0580 Bridge, Mahoning County, OH] [Satellite view] as of 10/16/2013.

23. Bing Maps (2013). [ATB-322-1917 Bridge, Ashtabula, OH] [Bird's eye view] as of 10/16/2013.
24. SIMULIA-ABAQUS (2013). 3DEXPERIENCE – PLM solutions, 3DCAD and simulation software.
25. Building Code Requirements for Structural Concrete (ACI 318-08) and Commentary (ACI, 2008). American Concrete Institute, Farmington Hills, MI.
26. American Association of State Highway and Transportation Officials (AASHTO, 2007). AASHTO LRFD Bridge Design Specifications SI Units (4th Edition). Washington, DC.
27. Paz, M. (1985). “Structural Dynamics, Theory & Computation”, Second Ed. ISBN: 0442275358, Nov. 13, 1985, Van Nostrand Reinhold Company, New York.
28. Cooley, J. W. and Tukey, J. W. (1965). “An Algorithm for the Machine Calculation of Complex Fourier Series”, American Mathematical Society, Mathematics of Computation, Vol. 19, No. 90, pp. 297–301.
29. Ren, W. and Zong, Z. (2003). “Output-only modal parameter identification of civil engineering structures”, Fuzhou University, China.
30. Federal Highway Administration (FHWA, 2011). “National Bridge Inventory General Condition Rating Guidance”, Bridge Preservation Guide, FHWA-HIF-11042.
31. Ewins, D. J. (2000). “Model Validation, Correlation for Updating”, Sadhana-Academy Proceedings in Engineering Sciences. Vol. 25, Part 3.

APPENDICES

APPENDIX A

Truck Axle Loads and Dimensions for Mahoning Bridge:



OHIO DEPARTMENT OF PUBLIC SAFETY
OHIO STATE HIGHWAY PATROL

Portable Scale Arrest and Weight Record

Date/Time of Violation _____ @ _____ Date/Time Vehicle Weighed 11-5-12 @ 0810
 Violation Occurred at _____ Distance Traveled _____
 Vehicle Weighed at ODOT BAILEY Rd County of Arrest _____
 Citation Number _____ Court Date _____ Total Fine Including Court Costs _____
 Driver Name _____ Operator License # _____ State _____
 Carrier Name ODOT Description of Load EMPTY
 Power Unit: Make INTL Model Year 99 Color WH Style of Vehicle NUMP
 Registration: Power Unit T4827 State _____ Trailer _____ State _____

Reasonable Suspicion for Traffic Stop (check all that apply)

Bulging Tires
 Visible Load
 Pulling Hard
 Slow Speed
 Insecure Load
 Vehicle Defect
 Oversize Load (5577.05)
 Registration Violation
 Other Violation _____

Axes	Axle Spacing	Scale #	Axle #	Left	Right	Axle #	Scale #	Total Weight
		<u>131</u>	Steer	<u>4,000</u>	<u>3,900</u>	Steer	<u>129</u>	<u>7,900</u>
1-2	<u>11-9</u>	<u>139</u>	2	<u>5,500</u>	<u>5,200</u>	2	<u>115</u>	<u>10,700</u>
1-3			3			3		
1-4			4			4		
1-5			5			5		
1-6			6			6		
1-7			7			7		
1-8			8			8		
1-9			9			9		
1-10			10			10		
1-11			11			11		

5577.04 (B) Maximum Gross Weight Allowed _____ lbs 5577.04 (D) Maximum Gross Weight Allowed _____ lbs

	Actual Weight in Pounds	Allowed Weight in Pounds	Number of Pounds Overweight	Issued Citation
Gross Weight	<u>18,600</u>	<u>40,000</u>		<input type="checkbox"/>
Axes 1	<u>7,900</u>	<u>20,000</u>		<input type="checkbox"/>
Axes 2	<u>10,700</u>	<u>20,000</u>		<input type="checkbox"/>
Inner-Bridge				<input type="checkbox"/>

Vehicle Length 11 Ft 9 In Vehicle Width 6 Ft 0 In Vehicle Height _____ Ft _____ In
 Arresting Officer _____ Unit _____ LLI Unit # 432 LLI Unit # _____
 Level Checked By 3022 Unit _____ All Scales Department of Agriculture Sealed Yes No
 Disposition of Vehicle: Axles shifted Vehicle off loaded Driven to closest safe haven to get legal
 Other (Explain) _____
 Check box for citations issued (check all that apply): Oversize IFTA Unsafe Permit Violation
 Other Arrest (List all) _____

OHP 0468 3/08 Page 1 of 2
(OSP-201.06)



OHIO DEPARTMENT OF PUBLIC SAFETY
OHIO STATE HIGHWAY PATROL

Portable Scale Arrest and Weight Record

Date/Time of Violation _____ @ _____ Date/Time Vehicle Weighed 11-5-12 @ 0746
 Violation Occurred at _____ Distance Traveled _____
 Vehicle Weighed at ODOT BAILEY RD County of Arrest _____
 Citation Number _____ Court Date _____ Total Fine Including Court Costs _____
 Driver Name _____ Operator License # _____ State _____
 Carrier Name ODOT Description of Load 1/2 LOAD
 Power Unit: Make INJL Model Year 07 Color WHI Style of Vehicle Dump
 Registration: Power Unit T4577 State _____ Trailer _____ State _____

Reasonable Suspicion for Traffic Stop (check all that apply)

- Bulging Tires Visible Load Pulling Hard Slow Speed Insecure Load Vehicle Defect
 Oversize Load (5577.05) Registration Violation Other Violation _____

Axles	Axle Spacing	Scale #	Axle #	Left	Right	Axle #	Scale #	Total Weight
1-2	<u>17-8</u>	<u>131</u>	Steer	<u>5,600</u>	<u>5,800</u>	Steer	<u>129</u>	<u>11,400</u>
1-3		<u>139</u>	2	<u>9,600</u>	<u>10,100</u>	2	<u>115</u>	<u>19,700</u>
1-4			3			3		
1-5			4			4		
1-6			5			5		
1-7			6			6		
1-8			7			7		
1-9			8			8		
1-10			9			9		
1-11			10			10		
			11			11		

5577.04 (B) Maximum Gross Weight Allowed _____ lbs 5577.04 (D) Maximum Gross Weight Allowed _____ lbs

	Actual Weight In Pounds	Allowed Weight In Pounds	Number of Pounds Overweight	Issued Citation
Gross Weight	<u>31,100</u>	<u>40,000</u>		<input type="checkbox"/>
Axles 1	<u>11,400</u>	<u>20,000</u>		<input type="checkbox"/>
Axles 2	<u>19,700</u>	<u>20,000</u>		<input type="checkbox"/>
Inner-Bridge				<input type="checkbox"/>

Vehicle Length 14 Ft 8 In Vehicle Width 6 Ft 0 In Vehicle Height _____ Ft _____ In
 Arresting Officer _____ Unit _____ LLI Unit # 432 LLI Unit # _____
 Level Checked By 3022 Unit _____ All Scales Department of Agriculture Sealed Yes No
 Disposition of Vehicle: Axles shifted Vehicle off loaded Driven to closest safe haven to get legal
 Other (Explain) _____
 Check box for citations issued (check all that apply): Oversize IFTA Unsafe Permit Violation
 Other Arrest (List all) _____



OHIO DEPARTMENT OF PUBLIC SAFETY
OHIO STATE HIGHWAY PATROL

Portable Scale Arrest and Weight Record

Date/Time of Violation _____ @ _____ Date/Time Vehicle Weighed 11-5-12 @ 0834
 Violation Occurred at _____ Distance Traveled _____
 Vehicle Weighed at ODOT BAILEY RD County of Arrest _____
 Citation Number _____ Court Date _____ Total Fine Including Court Costs _____
 Driver Name _____ Operator License # _____ State _____
 Carrier Name ODOT Description of Load FULL LOAD
 Power Unit: Make INTL Model Year 08 Color WHI Style of Vehicle Dump
 Registration: Power Unit T 4 946 State _____ Trailer _____ State _____

Reasonable Suspicion for Traffic Stop (check all that apply)

- Bulging Tires Visible Load Pulling Hard Slow Speed Insecure Load Vehicle Defect
 Oversize Load (5577.05) Registration Violation Other Violation _____

Axles	Axle Spacing	Scale #	Axle #	Left	Right	Axle #	Scale #	Total Weight
		<u>131</u>	Steer	<u>6,000</u>	<u>5,900</u>	Steer	<u>129</u>	<u>11,900</u>
1-2	<u>14-9</u>	<u>139</u>	2	<u>13,900</u>	<u>13,700</u>	2	<u>115</u>	<u>27,600</u>
1-3			3			3		
1-4			4			4		
1-5			5			5		
1-6			6			6		
1-7			7			7		
1-8			8			8		
1-9			9			9		
1-10			10			10		
1-11			11			11		

5577.04 (B) Maximum Gross Weight Allowed _____ lbs 5577.04 (D) Maximum Gross Weight Allowed _____ lbs

	Actual Weight In Pounds	Allowed Weight In Pounds	Number of Pounds Overweight	Issued Citation
Gross Weight	<u>39,500</u>	<u>40,000</u>		<input type="checkbox"/>
Axles 1	<u>11,900</u>	<u>20,000</u>		<input type="checkbox"/>
Axles 2	<u>27,600</u>	<u>20,000</u>		<input type="checkbox"/>
Inner-Bridge				<input type="checkbox"/>

Vehicle Length 14 Ft 9 In Vehicle Width 6 Ft 0 In Vehicle Height _____ Ft _____ In
 Arresting Officer _____ Unit _____ LLI Unit # 432 LLI Unit # _____
 Level Checked By 3022 Unit _____ All Scales Department of Agriculture Sealed Yes No
 Disposition of Vehicle: Axles shifted Vehicle off loaded Driven to closest safe haven to get legal
 Other (Explain) _____
 Check box for citations issued (check all that apply): Oversize IFTA Unsafe Permit Violation
 Other Arrest (List all) _____

Truck Axle Loads and Dimensions for Ashtabula Bridge:



OHIO DEPARTMENT OF PUBLIC SAFETY
OHIO STATE HIGHWAY PATROL

Portable Scale Arrest and Weight Record

Date/Time of Violation _____ @ _____ Date/Time Vehicle Weighed 11-13-12 @ 0828
 Violation Occurred at _____ Distance Traveled _____
 Vehicle Weighed at ODOT 512322 County of Arrest _____
 Citation Number _____ Court Date _____ Total Fine Including Court Costs _____
 Driver Name _____ Operator License # _____ State _____
 Carrier Name ODOT Description of Load EMPTY
 Power Unit: Make Intl Model Year 06 Color WHI Style of Vehicle Dump
 Registration: Power Unit T 4614 State OH Trailer _____ State _____

Reasonable Suspicion for Traffic Stop (check all that apply)

- Bulging Tires Visible Load Pulling Hard Slow Speed Insecure Load Vehicle Defect
 Oversize Load (5577.05) Registration Violation Other Violation _____

Axles	Axle Spacing	Scale #	Axle #	Left	Right	Axle #	Scale #	Total Weight
		<u>162</u>	Steer	<u>5,100</u>	<u>4,900</u>	Steer	<u>139</u>	<u>10,000</u>
1-2	<u>14-10</u>	<u>144</u>	2	<u>5,100</u>	<u>4,400</u>	2	<u>115</u>	<u>9,500</u>
1-3			3			3		
1-4			4			4		
1-5			5			5		
1-6			6			6		
1-7			7			7		
1-8			8			8		
1-9			9			9		
1-10			10			10		
1-11			11			11		

5577.04 (B) Maximum Gross Weight Allowed _____ lbs 5577.04 (D) Maximum Gross Weight Allowed _____ lbs

	Actual Weight in Pounds	Allowed Weight in Pounds	Number of Pounds Overweight	Issued Citation
Gross Weight	<u>19,500</u>	<u>40,000</u>		<input type="checkbox"/>
Axles 1	<u>10,000</u>	<u>20,000</u>		<input type="checkbox"/>
Axles 2	<u>9,500</u>	<u>20,000</u>		<input type="checkbox"/>
Inner-Bridge				<input type="checkbox"/>

Vehicle Length 14 Ft 10 In Vehicle Width 6 Ft 0 In Vehicle Height _____ Ft _____ In
 Arresting Officer _____ Unit _____ LLI Unit # 432 LLI Unit # _____
 Level Checked By 3022 Unit _____ All Scales Department of Agriculture Sealed Yes No
 Disposition of Vehicle: Axles shifted Vehicle off loaded Driven to closest safe haven to get legal
 Other (Explain) _____
 Check box for citations issued (check all that apply): Oversize IFTA Unsafe Permit Violation
 Other Arrest (List all) _____



OHIO DEPARTMENT OF PUBLIC SAFETY
OHIO STATE HIGHWAY PATROL

Portable Scale Arrest and Weight Record

Date/Time of Violation _____ @ _____ Date/Time Vehicle Weighed 11-13-12 @ 0824
 Violation Occurred at _____ Distance Traveled _____
 Vehicle Weighed at ODOT- 50322 County of Arrest _____
 Citation Number _____ Court Date _____ Total Fine Including Court Costs _____
 Driver Name _____ Operator License # _____ State _____
 Carrier Name ODOT Description of Load SALT - HALF LOAD
 Power Unit: Make INTL Model Year 05 Color WHI Style of Vehicle DAMP
 Registration: Power Unit T4947 State OH Trailer _____ State _____

Reasonable Suspicion for Traffic Stop (check all that apply)

- Bulging Tires Visible Load Pulling Hard Slow Speed Insecure Load Vehicle Defect
 Oversize Load (5577.05) Registration Violation Other Violation _____

Axles	Axle Spacing	Scale #	Axle #	Left	Right	Axle #	Scale #	Total Weight
		<u>162</u>	Steer	<u>5,500</u>	<u>5,500</u>	Steer	<u>139</u>	<u>11,000</u>
1-2	<u>14-10</u>	<u>144</u>	2	<u>7,800</u>	<u>8,300</u>	2	<u>115</u>	<u>16,100</u>
1-3			3			3		
1-4			4			4		
1-5			5			5		
1-6			6			6		
1-7			7			7		
1-8			8			8		
1-9			9			9		
1-10			10			10		
1-11			11			11		

5577.04 (B) Maximum Gross Weight Allowed _____ lbs 5577.04 (D) Maximum Gross Weight Allowed _____ lbs

	Actual Weight in Pounds	Allowed Weight in Pounds	Number of Pounds Overweight	Issued Citation
Gross Weight	<u>27,100</u>	<u>40,000</u>		<input type="checkbox"/>
Axles 1	<u>11,000</u>	<u>20,000</u>		<input type="checkbox"/>
Axles 2	<u>16,100</u>	<u>20,000</u>		<input type="checkbox"/>
Inner-Bridge				<input type="checkbox"/>

Vehicle Length 14 Ft 10 In Vehicle Width 6 Ft 0 In Vehicle Height _____ Ft _____ In
 Arresting Officer 432 Unit _____ LLI Unit # _____ LLI Unit # _____
 Level Checked By 3022 Unit _____ All Scales Department of Agriculture Sealed Yes No
 Disposition of Vehicle: Axles shifted Vehicle off loaded Driven to closest safe haven to get legal
 Other (Explain) _____
 Check box for citations issued (check all that apply): Oversize IFTA Unsafe Permit Violation
 Other Arrest (List all) _____



OHIO DEPARTMENT OF PUBLIC SAFETY
OHIO STATE HIGHWAY PATROL

Portable Scale Arrest and Weight Record

Date/Time of Violation _____ @ _____ Date/Time Vehicle Weighed 11-13-12 @ 0817
 Violation Occurred at _____ Distance Traveled _____
 Vehicle Weighed at ODOT- 52322 County of Arrest _____
 Citation Number _____ Court Date _____ Total Fine Including Court Costs _____
 Driver Name _____ Operator License # _____ State _____
 Carrier Name 962 ODOT Description of Load Full Load
 Power Unit: Make FNTL Model Year 04 Color WHITE Style of Vehicle Dump
 Registration: Power Unit T4942 State OH Trailer _____ State _____

Reasonable Suspicion for Traffic Stop (check all that apply)

- Bulging Tires Visible Load Pulling Hard Slow Speed Insecure Load Vehicle Defect
 Oversize Load (5577.05) Registration Violation Other Violation

Axles	Axle Spacing	Scale #	Axle #	Left	Right	Axle #	Scale #	Total Weight
1-2	14-9	<u>N02</u>	Steer	<u>6000</u>	<u>5300</u>	Steer	<u>139</u>	<u>11,300</u>
1-3		<u>194</u>	2	<u>10200</u>	<u>10800</u>	3	<u>115</u>	<u>21,000</u>
1-4			3			4		
1-5			4			5		
1-6			5			6		
1-7			6			7		
1-8			7			8		
1-9			8			9		
1-10			9			10		
1-11			10			11		

5577.04 (B) Maximum Gross Weight Allowed _____ lbs 5577.04 (D) Maximum Gross Weight Allowed _____ lbs

	Actual Weight in Pounds	Allowed Weight in Pounds	Number of Pounds Overweight	Issued Citation
Gross Weight	<u>32,300</u>	<u>40,000</u>		<input type="checkbox"/>
Axles 1	<u>11,300</u>	<u>20,000</u>		<input type="checkbox"/>
Axles 2	<u>21,000</u>	<u>20,000</u>		<input type="checkbox"/>
Inner-Bridge				<input type="checkbox"/>

Vehicle Length 14 Ft 9 In Vehicle Width 6 Ft 0 In Vehicle Height _____ Ft _____ In
 Arresting Officer _____ Unit _____ LLI Unit # 432 LLI Unit # _____
 Level Checked By 3022 Unit _____ All Scales Department of Agriculture Sealed Yes No
 Disposition of Vehicle: Axles shifted Vehicle off loaded Driven to closest safe haven to get legal
 Other (Explain) _____
 Check box for citations issued (check all that apply): Oversize IFTA Unsafe Permit Violation
 Other Arrest (List all) _____

Truck axle loads and dimensions for Trumbull Bridge:



OHIO DEPARTMENT OF PUBLIC SAFETY
OHIO STATE HIGHWAY PATROL

Portable Scale Arrest and Weight Record

Date/Time of Violation 09-27-13 @ NA Date/Time Vehicle Weighed 09-27-13 @ 1045
 Violation Occurred at SR 45 AT SR 88 Distance Traveled - 0 -
 Vehicle Weighed at SR 45/NORTH OF SR 88 County of Arrest TRUMBULL
 Citation Number NA Court Date NA Total Fine Including Court Costs NA
 Driver Name NA Operator License # NA State NA
 Carrier Name O.D.O.T. Description of Load GRINDINGS
 Power Unit: Make INTER Model Year 2012 Color WHITE Style of Vehicle DUMP
 Registration: Power Unit T 4823 State OHIO Trailer NA State NA

Reasonable Suspicion for Traffic Stop (check all that apply)

- Bulging Tires Visible Load Pulling Hard Slow Speed Insecure Load Vehicle Defect
 Oversize Load (5577.05) Registration Violation Other Violation XSU TEST

Axles	Axle Spacing	Scale #	Axle #	Left	Right	Axle #	Scale #	Total Weight
		<u>115</u>	Steer	<u>5,850</u>	<u>6,850</u>	Steer	<u>160</u>	<u>12,700</u>
1-2	<u>14.6</u>	<u>153</u>	2	<u>15,450</u>	<u>14,950</u>	2	<u>128</u>	<u>30,400</u>
1-3			3			3		
1-4			4			4		
1-5			5			5		
1-6			6			6		
1-7			7			7		
1-8			8			8		
1-9			9			9		
1-10			10			10		
1-11			11			11		

5577.04 (B) Maximum Gross Weight Allowed 40,000 lbs 5577.04 (D) Maximum Gross Weight Allowed 40,000 lbs

	Actual Weight in Pounds	Allowed Weight in Pounds	Number of Pounds Overweight	Issued Citation
Gross Weight	<u>43,100</u>	<u>40,000</u>	<u>3,100</u>	<input type="checkbox"/>
Axles				<input type="checkbox"/>
Axles REAR	<u>30,400</u>	<u>20,000</u>	<u>10,400</u>	<input type="checkbox"/>
Inner-Bridge				<input type="checkbox"/>

Vehicle Length ___ Ft ___ In Vehicle Width ___ Ft ___ In Vehicle Height ___ Ft ___ In
 Arresting Officer TR L.S. Woodward Unit 1673 LLI Unit # 3022 LLI Unit # _____
 Level Checked By 3022 Unit _____ All Scales Department of Agriculture Sealed Yes No
 Disposition of Vehicle: Axles shifted Vehicle off loaded Driven to closest safe haven to get legal
 Other (Explain) _____
 Check box for citations issued (check all that apply): Oversize IFTA Unsafe Permit Violation
 Other Arrest (List all) _____

APPENDIX B

Sample data collected under Half-loaded Truck at 25 mph

Sensor 1		Sensor 2		Sensor 3		Sensor 4	
Time, (msec)	Acceleration, (g)	Time, (msec)	Acceleration, (g)	Time, (msec)	Acceleration, (g)	Time, (msec)	Acceleration, (g)
0	-0.015625	0	-0.03125	0	-0.015625	0	-0.015625
10	0	10	0	9	-0.015625	10	0
20	-0.015625	20	0	19	-0.015625	20	-0.015625
30	-0.015625	30	-0.015625	29	-0.015625	30	-0.03125
40	-0.015625	40	-0.03125	39	-0.015625	40	-0.03125
50	-0.015625	50	0	49	0	50	-0.015625
60	0	60	-0.03125	59	0	60	-0.03125
70	-0.015625	70	0	69	-0.03125	70	-0.015625
80	-0.015625	80	0	79	-0.03125	80	-0.015625
90	0	90	0.015625	89	0.015625	90	-0.015625
100	-0.015625	100	0	99	0	100	-0.015625
110	0	110	0	109	0	110	0
120	-0.015625	120	0	119	0	120	-0.015625
130	0	130	0	129	0	130	-0.015625
140	-0.03125	140	-0.015625	139	0	140	-0.015625
150	0	150	0	149	-0.03125	150	-0.03125
166	0	160	0	160	0.015625	160	0.015625
170	0	171	0	170	-0.015625	170	-0.015625
180	-0.046875	180	-0.015625	180	0	183	-0.03125
190	-0.015625	190	0	189	0.015625	191	-0.015625
200	-0.03125	200	-0.015625	199	0	200	0
210	-0.015625	209	0	209	0	210	-0.015625
220	-0.015625	220	-0.015625	219	-0.015625	220	-0.015625
230	0	230	-0.015625	229	0	230	-0.046875
240	-0.015625	240	-0.015625	239	0	240	-0.03125
250	-0.03125	250	0	249	-0.015625	250	-0.015625
260	-0.03125	259	-0.015625	259	-0.015625	260	0
270	-0.03125	270	-0.015625	269	-0.015625	270	-0.015625
280	0	279	0	279	-0.015625	280	-0.046875
290	0	289	-0.015625	289	-0.015625	290	-0.015625
300	-0.015625	300	0	299	-0.015625	300	-0.015625
310	-0.03125	309	0	309	0	310	-0.03125
...
...

APPENDIX C

MAC Analysis

The amplitude values for Sensor 1 on both field and FE model bridges are:

$$N_1 = \begin{Bmatrix} 0.3938 \\ 0.3132 \\ 0.496 \\ 0.5818 \\ 0.2798 \\ 0.4349 \\ 0.6783 \\ 0.4818 \\ 0.373 \\ 0.492 \\ 0.6706 \\ 0.6876 \end{Bmatrix} \quad O_1 = \begin{Bmatrix} 0.7499 \\ 0.7403 \\ 0.6040 \\ 0.5717 \\ 0.7968 \\ 1.1896 \\ 1.0671 \\ 0.7756 \\ 0.856 \\ 1.1336 \\ 0.8125 \\ 2.1988 \end{Bmatrix}$$

$$N_1^T = \{0.3938 \ 0.3132 \ 0.4960 \ 0.5818 \ 0.2798 \ 0.4349 \ \dots \dots \dots \ 0.6876 \}$$

$$O_1^T = \{0.7499 \ 0.7403 \ 0.6040 \ 0.5717 \ 0.7968 \ 1.1896 \ \dots \dots \dots \ 2.1988 \}$$

The MAC value for Sensor 1 is calculated as follow:

$$MAC_1 = \frac{(N_1^T \cdot O_1^T)^2}{(N_1^T \cdot N_1) * (O_1^T \cdot O_1)}$$

$$MAC_1 = 0.866$$

The amplitude values for Sensor 4 on both field and FE model bridges are:

$$N_4 = \begin{Bmatrix} 0.4645 \\ 0.3591 \\ 0.6699 \\ 0.7699 \\ 0.3833 \\ 0.3730 \\ 0.7517 \\ 0.8603 \\ 0.3697 \\ 0.3349 \\ 0.5884 \\ 0.9250 \end{Bmatrix} \quad O_4 = \begin{Bmatrix} 0.7739 \\ 0.9640 \\ 0.7939 \\ 0.7475 \\ 1.0212 \\ 1.4836 \\ 1.6190 \\ 0.6671 \\ 0.9099 \\ 1.3405 \\ 1.0386 \\ 2.2605 \end{Bmatrix}$$

$$N_4^T = \{0.4645 \ 0.3591 \ 0.6699 \ 0.7699 \ 0.3833 \ 0.3730 \ \dots \dots \dots \ 0.9250 \}$$

$$O_4^T = \{0.7739 \ 0.9640 \ 0.7939 \ 0.7475 \ 1.0212 \ 1.4836 \ \dots \dots \dots \ 2.2605 \}$$

The MAC value for Sensor 4 is calculated as follow:

$$MAC_4 = \frac{(N_4^T \cdot O_4^T)^2}{(N_4^T \cdot N_4) * (O_4^T \cdot O_4)}$$

$$MAC_4 = 0.817$$

Reduction in fundamental frequency of Ashtabula Bridge between its newest and current conditions

The average fundamental frequency of the bridge at newest condition = 5.4464 Hz.

The average fundamental frequency of the bridge at current condition = 3.4383 Hz.

$$\begin{aligned} \text{Reduction in fundamental frequency of the bridge, } \Delta f &= \frac{5.4464 - 3.4383}{5.4464} * 100 \\ &= 36.87\% \end{aligned}$$

Theoretical fundamental frequency of Ashtabula Bridge at its newest condition

The fundamental frequency of the bridge at its newest condition can be found from the following equation:

$$f = 3.5608 * \sqrt{\frac{EI}{m_t L^3}}$$

Total mass of the bridge, $m_t = 2193.1 \frac{lb.s^2}{in}$

The length of the PSBB, $L = 1020 \text{ in}$.

The modulus of elasticity, E_c , for concrete is given by the following equation:

$$\begin{aligned} E_c &= 33 w_c^{1.5} \sqrt{f'_c} \\ E_c &= 33 * 150^{1.5} * \sqrt{5500} = 4496061 \text{ psi} \end{aligned}$$

The moment of Inertia, I , of the box beams was found as below:

$$I = \left(\frac{W_o H_o^3}{12} - \frac{W_i H_i^3}{12} \right) * n_b$$
$$I = \left(\frac{48 * 42^3}{12} - \frac{38 * 31.5^3}{12} \right) * 9$$
$$= 1776376 \text{ in}^4$$

Now, the fundamental frequency of the bridge can be calculated as follow:

$$f = 3.5608 * \sqrt{\frac{4496061 * 1776376}{2193.1 * 1020^3}} = 6.5963 \text{ Hz}$$

Difference in fundamental frequency of the bridge at its newest condition between FEA and theory

The fundamental frequency of the bridge at its newest condition from FEA is 5.4464 Hz.

The fundamental frequency of the bridge at its newest condition from theory is 6.5963 Hz.

The difference between the fundamental frequencies of the bridge found by FEA and Theory, Δf_{new} , is calculated as follow:

$$\Delta f_{\text{new}} = \frac{6.5963 - 5.4464}{6.5963} = 0.174$$

FEA Validation

1. Experimental Validation

The flexural rigidity of the bridge can be found from the following equation:

$$EI = \frac{f^2 * m_t * L^3}{3.5608^2}$$

For the bridge at its newest condition:

$$\begin{aligned} EI &= \frac{5.4464^2 * 2193.1 * 1020^3}{3.5608^2} \\ &= 5.444812 * 10^{12} \text{ lb. in}^2 \end{aligned}$$

For the bridge at its current condition:

$$\begin{aligned} EI^* &= \frac{3.4383^2 * 2193.1 * 1020^3}{3.5608^2} \\ &= 2.169958 * 10^{12} \text{ lb. in}^2 \end{aligned}$$

The MOE of the new bridge was calculated and equal to

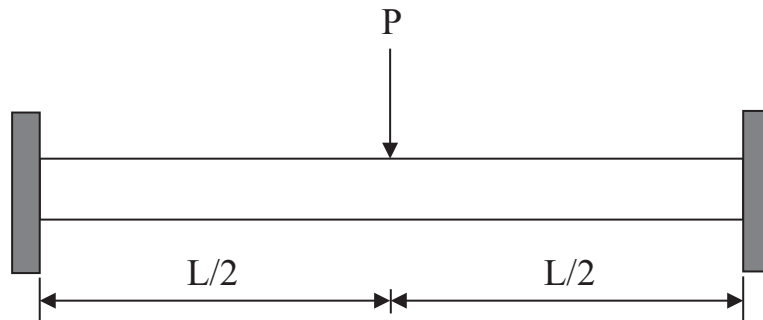
$$E_c = 4496061 \text{ psi}$$

The MOE of the current bridge, E_c^* , is calculated as follow:

$$\begin{aligned} E_c^* &= 4496061 * \frac{2.169958 * 10^{12}}{5.444812 * 10^{12}} \\ &= 1791846 \text{ psi} \end{aligned}$$

2. Theoretical Validation

The bridge was idealized as a beam with distributed mass and elasticity with fixed-fixed support, as shown in the following figure:



Approximate by hand calculations are performed for maximum stress, maximum deflection, and total mass of the bridge as follow:

2.1 Stress Calculation

The point load, P , at the middle of the bridge is calculated by multiplying the pressure by the area as follow:

$$P = 10 * (12 * 432) = 51840 \text{ lb}$$

For a fixed-fixed beam, the maximum stress, σ , at the middle of the span is given as follow:

$$\sigma_{max} = \frac{Mc}{I}$$

Where:

σ_{max} = stress at the middle of the beam, psi.

M = bending moment at the middle of the beam, lb.in.

C = distance from neutral axis of the box beams to the exterior fiber of box beams,
in.

I = moment of inertia of the box beams, in⁴.

The maximum moment at the middle of the span is calculated as:

$$M_{max} = \frac{PL}{8}$$

$$M_{max} = \frac{51840 * 1020}{8} = 6609600 \text{ lb.in}$$

Moment of inertia of the box beams is 1776376 in⁴.

The value of C is 21 in. for box beams of 42 in. deep.

By substituting these values into the equation of maximum stress, it produces

$$\sigma_{max} = \frac{6609600 * 21}{1776376} = 78.14 \text{ psi}$$

Maximum stress at the middle of the span from FEA was: $\sigma_{max} = 73 \text{ psi}$.

2.2 Deflection

Maximum deflection at the middle of the span is given as:

$$\Delta_{max} = \frac{PL^3}{192 EI}$$

$$\Delta_{max} = \frac{51840 * 1020^3}{192 * 4496060.776 * 1776375.563}$$

$$\Delta_{max} = 0.036 \text{ in.}$$

Maximum deflection at the middle of the span from FEA was: $\Delta_{max} = 0.05 \text{ in.}$

2.3 Total mass of the bridge

The total mass, m_t , of the bridge is calculated from its geometry and material property as follow:

$$\begin{aligned} m_t &= \frac{[(W_o H_o - W_i H_i) L n_b + W_i H_i t_d n_b n_d + 2W_i H_i t_e n_b + n_b W_o L t_w] * w_c}{12^3 * 386.4} \\ &= \frac{[(48 * 42 - 38 * 31.5) * 1020 * 9 + 9 * 48 * 1020 * 2.5] * 150}{12^3 * 386.4} \\ &\quad + \frac{[38 * 31.5 * 18 * 9 * 3 + 2 * 38 * 31.5 * 18 * 9] * 150}{12^3 * 386.4} \\ m_t &= 2154.321 \frac{\text{lb. s}^2}{\text{in}} \end{aligned}$$

The total mass of the bridge from FEA was: $m_t = 2193.1 \frac{\text{lb.s}^2}{\text{in}}$.